suggested to have a role in neuronal differentiation and neuronal survival (49), thus, TNF-α might inhibit neuronal differentiation. However, it is possible that other humoral factors potentially have the ability to induce dysfunction in neurogenesis.

Furthermore, MF projected from GCL neurons to CA3 pyramidal neurons were disturbed in slices exposed to HIV-1-infected MDM (Fig. 2, NFP). It is well known that the DG provides the main input to the hippocampus, and that neuronal information reaches the CA3 region through MF generated by GCL axons at the DG (23). It is also well known that the hippocampus plays an important role in learning and memory (23, 44). Our findings suggest that loss of MF with HIV-1 infection might explain the clinical observation that reduction in the ability to learn and form memory is frequently observed in HIV-1 encephalopathy patients.

In conclusion, the culture system that we report here reproduces the pathological changes of HIV-1 encephalopathy. Neuronal damage especially at the DG is induced by viral and/or host factors released from HIV-1-infected macrophages or activated microglial cells. Under the influence of these factors, the hippocampus can not recover from neuronal damage because neuronal progenitor cells can not differentiate into neurons and be incorporated into neuronal cell circuits. Finally, vulnerability of the DG might explain HIV-induced progressive pathological changes and reduction in the ability to learn and form memory in HIV-infected patients. As our data shows, this culture system will also be an adequate model to investigate and answer important questions regarding the involvement of host factors in HIV-1 encephalopathy. This system enables longitudinal studies in the pathology of HIV-1 encephalopathy, which is a great advantage of this *in vitro* model over existing *in vivo* models.

ACKNOWLEDGMENTS

We thank Naoko Misawa, Hiroshi Okada, Chuanyi Nie and Hiromu Yawo (Tohoku University) for helping with our study.

This work was supported by a Grant-in-Aid for Scientific Research on Priority Areas from the Ministry of Education, Culture, Sports, Sciences, and Technology of Japan and by grants for Research on HIV-AIDS and Health Science from the Ministry of Health, Labor, and Welfare of Japan.

REFERENCES

1. Ellis R., Langford D., Masliah E. (2007). HIV and antiretroviral therapy in the brain: neuronal injury and repair. *Nat. Rev. Neurosci* **8:** 33–44.
2. Gonzalez-Scarano F., Martin-Garcia J. (2005). The neuropathogenesis of AIDS. *Nat Rev Immunol* **5:** 69–81.
3. Price R.W., Brew B.J. (1988). The AIDS dementia complex. *J Infect Dis* **158:** 1079–83.
4. Dore G.J., Correll P.K., Li Y., Kaldor J.M., Cooper D.A., Brew B.J. (1999). Changes to AIDS dementia complex in the era of highly active antiretroviral therapy. *AIDS* **13:** 1249–53.
5. Sacktor N., McDermott M.P., Marder K., Schifitto G., Selnes O.A., McArthur J.C., Stern Y., Albert S., Palumbo D., Kieburtz K., De Marcaida J.A., Cohen B., Epstein L. (2002). HIV-associated cognitive impairment before and after the advent of combination therapy. *J Neurovirol* **8:** 136–42.
6. Mattson M.P., Haughey N.J., Nath A. (2005). Cell death in HIV dementia. *Cell Death Differ.* **12:** 893–904.
7. Kaul M., Garden G.A., Lipton S.A. (2001). Pathways to neuronal injury and apoptosis in HIV-associated dementia. *Nature* **410:** 988–94.
8. Minagar A., Shapshak P., Fujimura R., Ownby R., Heyes M., Eisdorfer C. (2002). The role of macrophage/microglia and astrocytes in the pathogenesis of three neurologic disorders: HIV-associated dementia, Alzheimer disease, and multiple sclerosis. *J Neurol Sci* **202:** 13–23.
9. Pulliam L., Herndier B.G., Tang N.M., McGrath M.S. (1991). Human immunodeficiency virus-infected macrophages produce soluble factors that cause histological and neurochemical alterations in cultured human brains. *J Clin Invest* **87:** 503–12.
10. Wang G.J., Chang L., Volkow N.D., Telang F., Logan J., Ernst T., Fowler J.S. (2004). Decreased brain dopaminergic transporters in HIV-associated dementia patients. *Brain* **127:** 2452–8.
11. Poluektova L., Meyer V., Walters L., Paez X., Gendelman H.E. (2005). Macrophage-induced inflammation affects hippocampal plasticity and neuronal development in a murine model of HIV-1 encephalitis. *Glia* **52:** 344–53.
12. Gahwiler B.H., Capogna M., Debanne D., McKinney R.A., Thompson S.M. (1997). Organotypic slice cultures: a technique has come of age. *Trends Neurosci* **20:** 471–7.
13. Dailey M.E., Buchanan J., Bergles D.E., Smith S.J. (1994). Mossy fiber growth and synaptogenesis in rat hippocampal slices in vitro. *J Neurosci* **14:** 1060–78.
14. Gahwiler B.H. (1984). Development of the hippocampus in vitro: cell types, synapses and receptors. *Neuroscience* **11:** 751–60.
15. Zimmer J., Gahwiler B.H. (1984). Cellular and connective organization of slice cultures of the rat hippocampus and fascia dentata. *J Comp Neurol* **228:** 432–46.
16. Gutierrez R., Heinemann U. (1999). Synaptic reorganization in explanted cultures of rat hippocampus. *Brain Res* **815:** 304–16.
17. Robain O., Barbin G., Billette de Villemeur T., Jardin L., Jahchan T., Ben-Ari Y. (1994). Development of mossy fiber synapses in hippocampal slice culture. *Brain Res Dev Brain Res* **80:** 244–50.
18. Kamada M., Li R.Y., Hashimoto M., Kakuda M., Okada H., Koyanagi Y., Ishizuka T., Yawo H. (2004). Intrinsic and spontaneous neurogenesis in the postnatal slice culture of rat hippocampus. *Eur J Neurosci* **20:** 2499–508.
19. Raineteau O., Rietschin L., Gradwohl G., Guillemot F., Gahwiler B.H. (2004). Neurogenesis in hippocampal slice cultures. *Mol Cell Neurosci* **26:** 241–50.
20. Koyanagi Y., O'Brien W.A., Zhao J.Q., Golde D.W., Gasson J.C., Chen I.S. (1988). Cytokines alter production of HIV-1 from primary mononuclear phagocytes. *Science* **241:** 1673–5.
21. An D.S., Morizono K., Li Q.X., Mao S.H., Lu S., Chen I.S. (1999). An inducible human immunodeficiency virus type 1 (HIV-1)

vector which effectively suppresses HIV-1 replication. *J Virol* **73:** 7671–7.
22. An D.S., Koyanagi Y., Zhao J.Q., Akkina R., Bristol G., Yamamoto N., Zack J.A., Chen I.S. (1997). High-efficiency transduction of human lymphoid progenitor cells and expression in differentiated T cells. *J Virol* **71:** 1397–404.
23. Nicoll R.A., Schmitz D. (2005). Synaptic plasticity at hippocampal mossy fibre synapses. *Nat Rev Neurosci* **6:** 863–76.
24. Lledo P.M., Alonso M., Grubb M.S. (2006). Adult neurogenesis and functional plasticity in neuronal circuits. *Nat Rev Neurosci* **7:** 179–93.
25. Aggoun-Zouaoui D., Charriaut-Marlangue C., Rivera S., Jorquera I., Ben-Ari Y., Represa A. (1996). The HIV-1 envelope protein gp120 induces neuronal apoptosis in hippocampal slices. *Neuroreport* **7:** 433–6.
26. Brana C., Biggs T.E., Mann D.A., Sundstrom L.E. (1999). A macrophage hippocampal slice co-culture system: application to the study of HIV-induced brain damage. *J Neurosci Methods* **90:** 7–11.
27. Prendergast M.A., Rogers D.T., Mulholland P.J., Littleton J.M., Wilkins L.H., Jr., Self R.L., Nath A. (2002). Neurotoxic effects of the human immunodeficiency virus type-1 transcription factor Tat require function of a polyamine sensitive-site on the N-methyl-D-aspartate receptor. *Brain Res* **954:** 300–7.
28. Williams K.C., Corey S., Westmoreland S.V., Pauley D., Knight H., deBakker C., Alvarez X., Lackner A.A. (2001). Perivascular macrophages are the primary cell type productively infected by simian immunodeficiency virus in the brains of macaques: implications for the neuropathogenesis of AIDS. *J Exp Med* **193:** 905–15.
29. Bachis A., Aden S.A., Nosheny R.L., Andrews P.M., Mocchetti I. (2006). Axonal transport of human immunodeficiency virus type 1 envelope protein glycoprotein 120 is found in association with neuronal apoptosis. *J Neurosci* **26:** 6771–80.
30. Bruce-Keller A.J., Chauhan A., Dimayuga F.O., Gee J., Keller J.N., Nath A. (2003). Synaptic transport of human immunodeficiency virus-Tat protein causes neurotoxicity and gliosis in rat brain. *J Neurosci* **23:** 8417–22.
31. Jones G.J., Barsby N.L., Cohen E.A., Holden J., Harris K., Dickie P., Jhamandas J., Power C. (2007). HIV-1 Vpr causes neuronal apoptosis and in vivo neurodegeneration. *J Neurosci* **27:** 3703–11.
32. Kaul M., Lipton S.A. (1999). Chemokines and activated macrophages in HIV gp120-induced neuronal apoptosis. *Proc Natl Acad Sci U S A* **96:** 8212–6.
33. Piller S.C., Jans P., Gage P.W., Jans D.A. (1998). Extracellular HIV-1 virus protein R causes a large inward current and cell death in cultured hippocampal neurons: implications for AIDS pathology. *Proc Natl Acad Sci U S A* **95:** 4595–600.
34. Fontana G., Valenti L., Raiteri M. (1997). Gp120 can revert antagonism at the glycine site of NMDA receptors mediating GABA release from cultured hippocampal neurons. *J Neurosci Res* **49:** 732–8.
35. Tenneti L., Lipton S.A. (2000). Involvement of activated caspase-3-like proteases in N-methyl-D-aspartate-induced apoptosis in cerebrocortical neurons. *J Neurochem* **74:** 134–42.
36. Adamson D.C., McArthur J.C., Dawson T.M., Dawson V.L. (1999). Rate and severity of HIV-associated dementia (HAD): correlations with Gp41 and iNOS. *Mol Med* **5:** 98–109.
37. Blond D., Raoul H., Le Grand R., Dormont D. (2000). Nitric oxide synthesis enhances human immunodeficiency virus replication in primary human macrophages. *J Virol* **74:** 8904–12.
38. Bukrinsky M.I., Nottet H.S., Schmidtmayerova H., Dubrovsky L., Flanagan C.R., Mullins M.E., Lipton S.A., Gendelman H.E. (1995). Regulation of nitric oxide synthase activity in human immunodeficiency virus type 1 (HIV-1)-infected monocytes: implications for HIV-associated neurological disease. *J Exp Med* **181:** 735–45.
39. Bezzi P., Domercq M., Brambilla L., Galli R., Schols D., De Clercq E., Vescovi A., Bagetta G., Kollias G., Meldolesi J., Volterra A. (2001). CXCR4-activated astrocyte glutamate release via TNFalpha: amplification by microglia triggers neurotoxicity. *Nat Neurosci* **4:** 702–10.
40. Foos T.M., Wu J.Y. (2002). The role of taurine in the central nervous system and the modulation of intracellular calcium homeostasis. *Neurochem Res* **27:** 21–6.
41. Haas C.A., Dudeck O., Kirsch M., Huszka C., Kann G., Pollak S., Zentner J., Frotscher M. (2002). Role for reelin in the development of granule cell dispersion in temporal lobe epilepsy. *J Neurosci* **22:** 5797–802.
42. Mayer D., Fischer H., Schneider U., Heimrich B., Schwemmle M. (2005). Borna disease virus replication in organotypic hippocampal slice cultures from rats results in selective damage of dentate granule cells. *J Virol* **79:** 11716–23.
43. Eriksson P.S., Perfilieva E., Bjork-Eriksson T., Alborn A.M., Nordborg C., Peterson D.A., Gage F.H. (1998). Neurogenesis in the adult human hippocampus. *Nat Med* **4:** 1313–7.
44. Shors T.J., Miesegaes G., Beylin A., Zhao M., Rydel T., Gould E. (2001). Neurogenesis in the adult is involved in the formation of trace memories. *Nature* **410:** 372–6.
45. van Praag H., Schinder A.F., Christie B.R., Toni N., Palmer T.D., Gage F.H. (2002). Functiona neurogenesis in the adult hippocampus. *Nature* **415:** 1030–4.
46. McKinney R.A., Capogna M., Durr R., Gahwiler B.H., Thompson S.M. (1999). Miniature synaptic events maintain dendritic spines via AMPA receptor activation. *Nat Neurosci* **2:** 44–9.
47. Nacher J., McEwen B.S. (2006). The role of N-methyl-D-asparate receptors in neurogenesis. *Hippocampus* **16:** 267–70.
48. Nacher J., Varea E., Miguel Blasco-Ibanez J., Gomez-Climent M.A., Castillo-Gomez E., Crespo C., Martinez-Guijarro F.J., McEwen B.S. (2007). N-methyl-d-aspartate receptor expression during adult neurogenesis in the rat dentate gyrus. *Neuroscience* **144:** 855–64.
49. Horton A.C., Ehlers M.D. (2003). Neuronal polarity and trafficking. *Neuron* **40:** 277–95.

JOURNAL OF VIROLOGY, Mar. 2008, p. 2528–2542 Vol. 82, No. 5
0022-538X/08/$08.00+0 doi:10.1128/JVI.02094-07

Human Immunodeficiency Virus Type 1 Vpr Inhibits Axonal Outgrowth through Induction of Mitochondrial Dysfunction▽

Hiroko Kitayama,[1] Yoshiharu Miura,[1] Yoshinori Ando,[1] Shigeki Hoshino,[2,3] Yukihito Ishizaka,[2] and Yoshio Koyanagi[1]*

Laboratory of Viral Pathogenesis, Institute for Virus Research, Kyoto University, Kyoto 606-8507, Japan[1]; Department of Intractable Diseases, International Medical Center of Japan, Tokyo 162-8655, Japan[2]; and Graduate School of Comprehensive Human Sciences, University of Tsukuba, Tsukuba 305-8577, Japan[3]

Received 21 September 2007/Accepted 12 December 2007

Human immunodeficiency virus type 1 (HIV-1)-infected macrophages damage mature neurons in the brain, although their effect on neuronal development has not been clarified. In this study, we show that HIV-1-infected macrophages produce factors that impair the development of neuronal precursor cells and that soluble viral protein R (Vpr) is one of the factors that has the ability to suppress axonal growth. Cell biological analysis revealed that extracellularly administered recombinant Vpr (rVpr) clearly accumulated in mitochondria where a Vpr-binding protein adenine nucleotide translocator localizes and also decreased the mitochondrial membrane potential, which led to ATP synthesis. The depletion of ATP synthesis reduced the transportation of mitochondria within neurites. This mitochondrial dysfunction inhibited axonal growth even when the frequency of apoptosis was not significant. We also found that point mutations of arginine (R) residues to alanine (A) residues at positions 73, 77, and 80 rendered rVpr incapable of causing mitochondrial membrane depolarization and axonal growth inhibition. Moreover, the Vpr-induced inhibition was suppressed after treatment with a ubiquinone analogue (ubiquinone-10). Our results suggest that soluble Vpr is a major viral factor that causes a disturbance in neuronal development through the induction of mitochondrial dysfunction. Since ubiquinone-10 protects the neuronal plasticity in vitro, it may be a therapeutic agent that can offer defense against HIV-1-associated neurological disease.

AIDS patients who have high levels of viral loads in the cerebrospinal fluid (CSF) tend to develop human immunodeficiency virus (HIV)-associated dementia (14, 31). Recently, attention has been brought to milder neurological diseases displayed in the antiretrovirus therapy-treated patients and healthy HIV-infected individuals (50). Mild neurocognitive disorder is defined as the presence of several cognitive deficits (14). In histopathological examinations of autopsy samples of HIV-1-infected brains, apoptosis in neurons was frequently found (2, 19). However, the frequency of apoptosis was low in patients displaying the milder neurological diseases (1). Although the molecules involved in HIV-associated neurological disturbance have not been completely identified, many data indicate that HIV type 1 (HIV-1)-infected macrophages or microglial cells produce neurotoxic factors such as viral products, excitotoxins, and/or cytokines (14, 20).

Viral proteins that are released from HIV-1-infected macrophages or microglial cells can be deleterious to the central nervous system (CNS). HIV-1 envelope glycoprotein 120 (gp120), transcriptional transactivator (Tat), and viral protein R (Vpr) have been shown to be toxic to neurons (14, 20). Recently, it has been reported that the HIV-1-induced inflammation caused by infiltrated macrophages might impede neuronal cell development in the hippocampus, as shown by a murine model of HIV-1 encephalopathy (43). However, it has not been shown that a viral protein released from HIV-1-infected macrophages can cause the retardation of neuronal development.

An HIV-1 accessory protein, Vpr, which is synthesized late in the HIV-1 replication cycle, is present in a soluble form in CSF and sera of HIV-1-infected patients displaying neurological disorders (34). It has been shown that Vpr causes many cellular dysfunctions, including cell cycle arrest at the G_2 phase caused by the induction of the damage-specific DNA-binding protein 1 (DDB1) and the Cullin 4A (Cul4A) E3 ubiquitin ligase pathway (8, 12, 13, 24, 33, 51, 56, 59) and the induction of caspase-dependent apoptosis (39). It is thought that HIV-1 Vpr is a potentially toxic molecule to mature neurons. In vitro studies using cultured neurons derived from rat hippocampal, cortical, and striatal neurons (42, 49) and an in vivo study using Vpr transgenic mice have shown that HIV-1 Vpr might have the potential to cause neuronal apoptosis (27). Furthermore, it is also known that Vpr-induced apoptosis is mediated by its binding to the adenine nucleotide translocator (ANT) in the inner membrane of mitochondria (25, 26, 48).

It has been shown that mitochondria play important roles in the establishment of axonal polarity and the regulation of neurite outgrowth during neuronal development (36). The trafficking of mitochondria may be a necessary task in neuronal development (10). However, the influence of HIV-1 Vpr on immature neurons, including neuronal progenitor cells, or its effect on neuronal plasticity has not been clarified.

Many pieces of evidence indicate that active neurogenesis occurs in parts of the adult brain, including the dentate gyrus (DG) of the hippocampus, the olfactory bulb, and the ventric-

* Corresponding author. Mailing address: Laboratory of Viral Pathogenesis, Institute for Virus Research, Kyoto University, 53 Shogoinkawara-cho, Sakyo-ku, Kyoto 606-8507, Japan. Phone: 81-75-751-4811. Fax: 81-75-751-4812. E-mail: ykoyanag@virus.kyoto-u.ac.jp.

▽ Published ahead of print on 19 December 2007.

ular epithelium, and is crucial for the formation of neuronal plasticity (35). Neural stem cells derived from DG differentiate into neurons and form synaptic networks, and these morphological and physiological features strongly suggest that the new neurons are incorporated into the hippocampal local circuitry and that they are involved in hippocampus-dependent memory formation and brain repair (35, 53, 57). The goal of this study was to identify the factors that damage neuronal development and to reveal the mechanisms of the inhibition of neuronal development that might cause the pathological alterations of HIV encephalopathy, including cognitive impairment in both pediatric patients and adult patients.

In this study, we examine whether HIV-1-infected macrophages inhibit neuronal cell development by using precursor cells isolated from murine fetal brain tissue. We discovered that soluble Vpr is one of the inhibitory factors of axonal growth and that it delays differentiation in precursor cells. Moreover, a subsequent detailed analysis of recombinant Vpr (rVpr)-treated cells revealed Vpr-induced mitochondrial membrane depolarization, which resulted in the disruption of ATP synthesis and the inhibition of mitochondrial transport in neurites of neuronal precursor cells. These negative effects were significantly suppressed in differentiation cultures and organotypic hippocampal slice cultures by ubiquinone-10 (UQ), which is a ubiquinone analogue that protects mitochondria from membrane depolarization. These data suggest that UQ is a therapeutic agent that can offer defense against the HIV-1-induced impairment of neuronal development.

MATERIALS AND METHODS

Preparation of CM from MDM. Neurobasal conditioned medium (CM) supplemented with Dulbecco's modified Eagle's medium (DMEM)-high glucose, 10% fetal calf serum, and B27 supplement (Invitrogen, Carlsbad, CA) was used to culture monocyte-derived macrophages (MDM) isolated from peripheral blood mononuclear cells of HIV-1-seronegative healthy donors. The MDM were left uninfected or were infected with HIV-1_{JRFL} (32) at a multiplicity of infection of 1.0. Five days after HIV-1 infection, culture supernatant was collected and the concentration of $p24^{CA}$ antigen (RETROtek; ZeptoMetrix, Buffalo, NY) and soluble Vpr protein (23) in each CM was measured by enzyme-linked immunosorbent assay (ELISA). Control CM, CM collected from uninfected MDM, and CM collected from infected MDM were designated C-CM, M-CM, and HIV-CM, respectively.

Preparation of rVpr and synthesized peptides. Wild-type rVpr (rVpr-WT) was purified as described previously (54). Three rVpr mutants that had alanine (A) instead of arginine (R) at position 80 (R80A), isoleucine (I) at position 81 (I81A), or arginine at positions 73, 77, and 80 (R73, 77, 80A) were prepared with the same procedure as that used for rVpr-WT. Four Vpr peptides were synthesized (Osaka Peptide Institute, Japan, and Wako Pure Chemicals, Japan).

Differentiation culture of neurons. The generation and maintenance of neurospheres from murine embryonic forebrains were performed as described previously (16). Briefly, cells were dissociated from the forebrains of embryonic day 15 ICR mice (Japan SLC, Inc., Japan). The experiments were carried out in accordance with the guidelines for animal experimentation at Kyoto University. Three days after the initiation of culture, neurospheres were separated into individual cells by trypsin-EDTA treatment and were plated onto glass coverslips (12 mm) precoated with poly-L-ornithine hydrochloride (Sigma-Aldrich, St. Louis, MO) and laminin from Engelbreth-Holm-Swarm murine sarcoma (Sigma-Aldrich) and were cultured with neurobasal CM. Phase-contrast images were acquired using a Leica CTR 6500 (Leica Microsystems, Heidelberg, Germany) with 20× and 40× objectives.

Measurement of neurite length and classification of developmental stages. Quantifications were performed using Leica FW4000 software (Leica Microsystems). To measure the length of neurites or axons, each neurite or axon from randomly chosen cells was traced manually from the proximal end to the distal end. To determine the percentage of cells in each developmental stage, randomly chosen cells were classified into three developmental stages based on their morphologies. Any progenitor cells that had an extended neurite (at least twice as long as other neurites by observation) were categorized as stage 3, and progenitor cells that do not have an extended neurite were categorized as stage 2. Progenitor cells that formed lamellipodia, which form small protrusion veils and a few spikes, were categorized as stage 1. The samples were prepared and blinded by one investigator. The measurement and classification were done by another investigator, to whom no information regarding the treatments was given. Experiments were repeated at least three times, and more than 100 adherent progenitor cells were analyzed for each independent experiment.

Vpr neutralization. To neutralize soluble Vpr in HIV-CM, progenitor cells were cultured in HIV-CM supplemented with mouse monoclonal anti-Vpr antibody (8D1; 260 ng/ml) (23) or mouse monoclonal anti-$p17^{MA}$ antibody (260 ng/ml; Advanced Biotechnologies, Columbia, MD).

Reagents. The following reagents were used: caspase-3 inhibitor (z-DEVD-fmk; BD Biosciences, San Diego, CA), UQ (Sigma-Aldrich), ATP (Sigma-Aldrich), and carbonyl cyanide 4-(trifluoromethoxy) phenylhydrazone (FCCP; Sigma-Aldrich).

Staining of mitochondria in live cells. To visualize mitochondria and calculate the velocity of mitochondrial transport in neurites or axons, cells were incubated with 100 nM MitoTracker Green FM (Invitrogen) by following the manufacturer's protocol. The temperature was maintained at 37°C with an air stream incubator. Cells were visualized with an oil immersion 63× objective on a confocal laser microscope (TCS SP2 AOBS; Leica Microsystems) using a 488-nm excitation wavelength for the quantification of mean pixels. The quantification of mean pixels was done by following the protocol supplied by the manufacturer (LCS Lite software; Leica Microsystems). To measure the velocity, images were acquired using a fluorescence microscope (Leica CTR 6500) using a green fluorescent protein (GFP) filter every 10 s for 120 s. The velocity of mitochondrial transport within neurites or axons was calculated by displacement (in micrometers) over time (in seconds). The mitochondrial membrane potential ($\Delta\Psi m$) was calculated using the fluorescent intensity of a $\Delta\Psi m$-sensitive dye, 5,5′,6,6′-tetrachloro-1,1′,3,3′-tetraethylbenzimidazolyl-carbocyanine iodide (JC-1; Invitrogen), by following the manufacturer's protocol. At 48 h of culture, cells were incubated with 1 μg/ml JC-1 at 37°C for 30 min and were visualized with an oil immersion 63× objective on a fluorescence microscope (Leica CTR 6500) using GFP and Texas Red filters. The temperature was maintained at 37°C with an air stream incubator. The red fluorescence intensity and green fluorescence intensity were measured using Leica FW4000 software. The normalized intensity ratio between green and red depends on $\Delta\Psi m$. $\Delta\Psi m$ (normalized JC-1 ratio) was calculated with the following formula: $\Delta\Psi m$ = (red fluorescence intensity − base fluorescence intensity)/(green fluorescence intensity − base fluorescence intensity).

ATP production assay. Cellular ATP levels were measured using the ATP bioluminescence assay kit HS II (Roche Applied Sciences, Indianapolis, IN). Briefly, cells were lysed in cell lysis reagent. Cell lysate and luciferase reagent then were added to microplates, and the luminescence was measured using a WALLAC ARVO SX 1420 multilabel counter (Perkin Elmer). The standard curve for ATP was obtained by measuring the luciferase intensity from a serially diluted standard ATP solution.

Isolation of mitochondria and Western blotting. The isolation of mitochondria in neuronal cells left untreated or treated with rVpr for 48 h was performed with the Qproteome mitochondria isolation kit (Qiagen, Hilden, Germany) by following the manufacturer's protocol. The cytosolic fraction was concentrated by acetone precipitation. Proteins from the mitochondrial fraction or cytosolic fraction or the whole-cell lysate were separated by sodium dodecyl sulfate–15% polyacrylamide gel electrophoresis, transferred onto a polyvinyl difluoride membrane (Immobilon transfer membranes; Millipore, Bedford, MA), and incubated with antibodies against cytochrome *c* (BD Biosciences), Vpr (23), and ANT (Santa Cruz Biotechnology, Santa Cruz, CA). Anti-mouse/rabbit immunoglobulin G (IgG) horseradish peroxidase-linked antibody (Cell Signaling Technology, Denver, MA) was used to detect the primary antibodies bound to the protein by using Western lighting chemiluminescence reagent (Perkin Elmer LAS, Boston, MA).

Slice cultures and retrovirus vector transduction. Organotypic hippocampal slices were prepared from postnatal 7-day-old Wistar Hannover GALAS rats (CLEA Japan, Inc.) as previously described (28). The slices were cultured on a porous translucent membrane (Millicell-CM; Millipore) at 34°C for 14 days. Slices were cocultured with HIV-1_{JRFL}-infected cells (multiplicity of infection, 1.0), uninfected MDM, or recombinant Vpr protein (23) across the porous membrane for 2 weeks. In some slices, an enhanced GFP (EGFP)-expressing murine leukemia virus (MLV)-based vector, SRα-EGFP (3), was inoculated in the suprapyramidal region of the dentate granule cell layer (GCL).

Immunocytochemistry and immunohistochemistry. The neuronal cells were fixed with paraformaldehyde (PFA) for 1 h at 4°C. After being washed, fixed cells were treated with phosphate-buffered saline (PBS) containing 5% normal goat serum (NGS) and 0.05% Triton X-100 at room temperature (RT) for 1 h, followed by incubation with mouse monoclonal anti-cytochrome *c* at RT for 2 h. Samples then were incubated with Alexa Fluor 488-conjugated anti-mouse IgG (Invitrogen) at RT for 2 h. Nuclei were stained using Hoechst 33342 (Invitrogen). The slices were fixed by immersion in 4% PFA for 1 h at 4°C. After being washed, slices were treated with buffer containing 5% NGS and 0.3% Triton X-100 (blocking solution) at 4°C overnight and then incubated with the following primary mouse monoclonal antibodies: anti-β-3-tubulin (B3T; Monosan, Uden, The Netherlands), neurofilament protein (NFP; DakoCytomation, Carpinteria, CA), microtubule-associated protein 2 (MAP2; Upstate, Lake Placid, NY), and neuronal nuclei (NeuN; Chemicon, Temecula, CA) at 4°C overnight in blocking solution. Samples subsequently were incubated at RT for 6 h with a fluorescent dye-conjugated secondary antibody (Alexa Fluor 594- or 488-conjugated anti-mouse IgG [Invitrogen]). Each sample was examined under a confocal laser microscope (TCS SP2 AOBS) with 40× and 63× objectives. The quantification of fluorescence intensity was done by following the protocol supplied by the manufacturer.

Statistical analysis. Data were generated from at least three replicate experiments. The statistical analysis was carried out by one-way analysis of variance. Multiple comparisons were performed with the Student's *t* test. A *P* value of less than 0.05 was considered significant.

RESULTS

Inhibition of axonal growth by HIV-1-infected MDM. To examine the effect of HIV-1-infected macrophages on neuronal development in vitro, we utilized differentiation cultures using neuronal progenitors derived from murine neurosphere cells. Neurite outgrowth in neurosphere cells apparently was hampered in the presence of CM of HIV-1_{JRFL}-infected MDM (HIV-CM) compared to the growth of those cultured in CM of uninfected MDM (M-CM) or in control CM (C-CM) (Fig. 1A). A similar inhibition was observed when we used progenitor cells isolated from murine fetal brain (data not shown). At 8 h of culture, the mean lengths of primary neurites were comparable among progenitor cells cultured in HIV-CM, M-CM, and C-CM (26.15 ± 8.94, 33.95 ± 4.84, and 34.90 ± 13.11 μm, respectively) (Fig. 1B), indicating that the initial steps of neurite generation are not affected. At 24 h of culture, however, the mean length of primary neurites in progenitor cells cultured in HIV-CM was less than those in progenitor cells cultured in M-CM or C-CM. As shown in Fig. 1B, at 72 h, the average length of the primary neurites of neuronal cells cultured with HIV-CM (52.20 ± 14.64 μm) was approximately one-third the length of those from cells cultured with M-CM or C-CM (169.70 ± 37.52 and 175.15 ± 34.14 μm, respectively).

We then evaluated polarity formation in progenitor cells cultured in HIV-CM, M-CM, and C-CM. When neuronal progenitor cells are plated, they initially form lamellipodia, which form small protrusion veils and a few spikes (stage 1). Following this event, several neurites of similar lengths extend (stage 2), leading to the formation of minor neurites. Finally, one of the neurites starts to grow rapidly, forming the primary neurite, while other neurites remain quiescent. This step is characterized by primary neurite outgrowth and axon formation, which results in the morphological polarization of the neuron (stage 3) (22). One hundred cells were randomly chosen from each CM and were classified into the three developmental stages according to their morphologies. When the progenitor cells were examined at 24 h, we found that more than half of them were in stage 2, independent of the CM (Fig. 1C). As shown in Fig. 1D, at 48 h the majority of progenitors cultured in C-CM and M-CM were in stage 3 (63.33% ± 0.58% and 55.33% ± 8.49%, respectively), but the majority of them were still in stage 2 in HIV-CM (64.00% ± 6.36%). These results indicate that the cells exposed to C-CM and M-CM had similar abilities to differentiate up to 72 h in culture and that the differentiation of HIV-CM-cultured progenitors was arrested at stage 2.

When HIV-CM with a low p24 concentration (below 200 pg/ml) was used, the inhibition of axon formation was not observed at 48 h (data not shown). However, when HIV-CM with a high HIV-1 p24 concentration (70.28 ± 21.6 ng/ml) was used, the inhibition was obvious, indicating the possibility that viral proteins are involved in the inhibition of axon formation. In fact, a relatively large amount of Vpr was detected in HIV-1 virion-free supernatant of HIV-CM (18.37 ± 7.54 pg/ml), as measured using ELISA. When the progenitor cells were cultured in HIV-CM in the presence of anti-Vpr antibody (8D1) (23), neurite outgrowth was clearly rescued at 72 h (Fig. 1E) and the number of neuronal cells scored at stage 3 clearly increased (Fig. 1F). On the other hand, no protective effect was observed in the anti-$p17^{MA}$ antibody-treated groups (Fig. 1E and F). These results suggest that Vpr produced from HIV-1-infected MDM played a role in the inhibition of axonal growth. As the recovery of neuronal cell differentiation was not complete, HIV-CM likely contains another inhibitory factor(s) against neurite outgrowth.

Inhibition of axonal outgrowth by soluble Vpr. To assess the direct effect of Vpr on axon formation, rVpr (23) was added to differentiation cultures of mouse neurosphere-dissociated progenitor cells. Since the highest concentration of soluble Vpr protein in HIV-1 virion-free HIV-CM was 26.60 pg/ml (1.9 pM) as measured using ELISA, rVpr was used at two concentrations: 2.0 pM (approximately equal to the highest concentration of Vpr in HIV-CM, designated Vpr-2.0) and 10 pM (Vpr-10). The progenitor cells were cultured in CM containing rVpr and were analyzed for neurite outgrowth. Neurite outgrowth was clearly inhibited in a dose-dependent manner (Fig. 2A and B). As shown in Fig. 2B, at 72 h in culture, the mean length of primary neurites was 176.70 ± 13.75 μm (C-CM), 105.97 ± 6.28 μm (Vpr-2.0), and 85.83 ± 17.46 μm (Vpr-10) (Fig. 2B). When anti-Vpr antibody was added to the culture prior to the addition of rVpr, Vpr-induced inhibition of neurite outgrowth was clearly blocked (percentage of suppression, 68.50%; no statistical significance was found compared to results for the control group) (Fig. 2C).

To examine whether Vpr inhibits axon and neuronal polarity formation, progenitor cells were plated and cultured in the presence of C-CM, Vpr-2.0, or Vpr-10. We randomly selected 100 cells in each culture and classified them into the three developmental stages. At 24 h, more than half of them were in stage 2, independent of the CM (Fig. 2D). At 48 h, the percentage of stage 3 progenitor cells was 64.9% ± 2.62% in cells cultured with C-CM, while the percentage was significantly lower in the presence of rVpr (Vpr-2.0, 29.67% ± 4.04%; Vpr-10, 28.00% ± 3.00%). A considerably large fraction of cells remained in stage 2 (Vpr-2.0, 64.33% ± 1.53%; Vpr-10, 63.33% ± 3.21%) when exposed to rVpr (Fig. 2E). These results confirm that the soluble form of Vpr protein induces

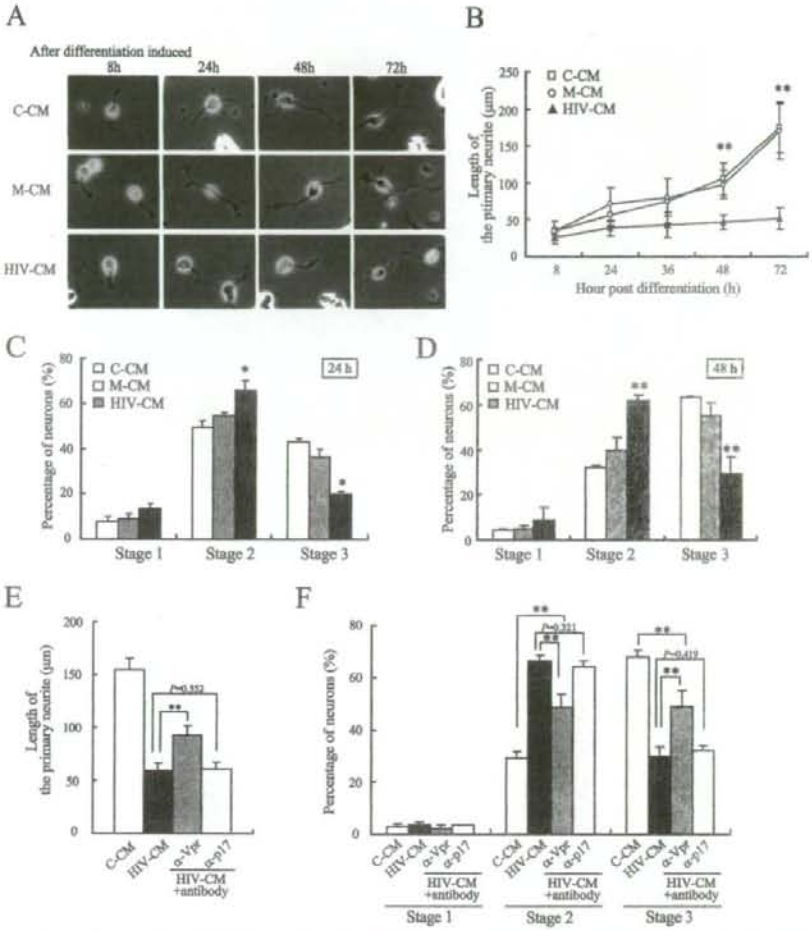

FIG. 1. Impairment of axonal growth by HIV-1-infected MDM. (A) The neurite outgrowth of neurons cultured in C-CM, M-CM, or HIV-CM was monitored for 72 h in differentiation cultures of neuronal progenitor cells. Phase-contrast images were obtained using a 40× objective. Scale bars, 20 μm. (B) The length of the primary neurite of each cell was measured in the culture. **, $P < 0.01$ compared to results for C-CM and M-CM cultures. (C and D) Progenitor cells under each condition were classified into three developmental stages as described in Materials and Methods at 24 h (C) and 48 h (D) in culture. *, $P < 0.05$ compared to results for C-CM and M-CM cultures. (E) Progenitor cells were cultured with C-CM, HIV-CM, or HIV-CM supplemented with anti-Vpr antibody (260 ng/ml; HIV-CM+anti-Vpr) or anti-$p17^{MA}$ antibody (260 ng/ml; HIV-CM+anti-p17), and the length of the primary neurite was measured. **, $P < 0.01$. (F) The cells under each condition were classified into three developmental stages. **, $P < 0.01$.

the inhibition of axon formation in a manner similar to that of HIV-CM.

Mitochondrial membrane depolarization of neurons caused by Vpr. Mitochondria play important roles in neuronal developmental processes, including the establishment of axon polarity and the regulation of neurite outgrowth (36, 37). Since it has been reported that Vpr influences mitochondrial function in several cell types and induces mitochondrial membrane depolarization (5, 25, 26), Vpr also may induce mitochondrial dysfunction in neuronal progenitor cells. To elucidate the mechanism of Vpr-induced mitochondrial dysfunction, we added serially increasing concentrations of rVpr, from 0.2 pM to 1.0 nM, to progenitor cell cultures and measured the $\Delta\Psi m$ in live neuronal progenitor cells using staining with JC-1. As shown in Fig. 3A, the $\Delta\Psi m$ clearly decreased in rVpr-treated cells in a dose-dependent manner, indicating that Vpr also affected the $\Delta\Psi m$ in neuronal progenitor cells.

Mitochondrial membrane depolarization has been shown to reduce ATP production (10). The proper transport of mitochondria within axons or neurites needs its motor proteins, and the motor proteins utilize ATP for its mobilization (10, 21). As shown in Fig. 3B, the concentration of cellular ATP was significantly reduced by exposure to 2.0 pM rVpr (1.50 ± 0.56 μM) compared to that in C-CM-cultured progenitor cells (4.57 ± 0.79 μM).

Although mitochondrial membrane depolarization and the

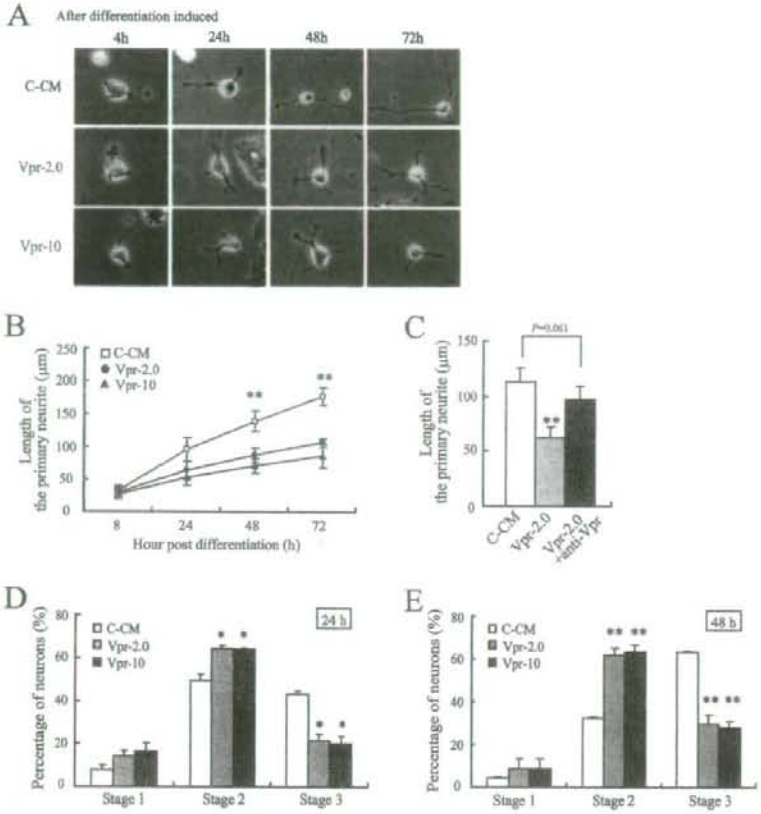

FIG. 2. Axonal malformation by Vpr in neuronal cells. (A) C-CM, Vpr-2.0, and Vpr-10 were used in differentiation cultures of neuronal progenitor cells, and neurite outgrowth was monitored for 72 h. Phase-contrast images were obtained using a 40× objective. Scale bars, 20 μm. (B) The lengths of the primary neurites of the neurons were measured. **, $P < 0.01$ compared to results for C-CM culture. (C) The length of the primary neurites of neurons cultured with C-CM, Vpr-2.0, or rVpr together with anti-Vpr antibody (Vpr-2.0+anti-Vpr) were measured. **, $P < 0.01$ compared to results for culture with C-CM or Vpr-2.0+anti-Vpr. (D and E) Progenitor cells under each condition were classified into three developmental stages at 24 h (D) and 48 h (E) in culture as described above. **, $P < 0.01$ compared to results for C-CM culture.

depletion of ATP concentration were induced by rVpr treatment, there was no significant difference in the percentages of progenitor cells expressing activated caspase-3 between 2.0 pM rVpr-treated cells and C-CM-treated cells (Table 1). Although apoptosis was not detected in progenitor cells cultured with low concentrations of rVpr (0.2, 2.0, and 10 pM), at higher concentrations of rVpr (100 pM or 1.0 nM), the differentiation of progenitor cells was arrested at stage 1 or early in stage 2 (data not shown), and many cells expressed activated caspase-3 (Table 1).

It has been shown that the depolarization of the mitochondrial membrane potential and the inhibition of ATP synthesis cause mitochondrial transport to slow down (10, 46). To measure the velocity of mitochondrial movement within neurites or axons, progenitor cells left untreated or treated with rVpr were stained for mitochondria using MitoTracker. We detected severely suppressed mitochondrial transport within neurites in 2.0 pM rVpr-treated cells (Fig. 3C, column b) compared to that of neurites cultured in C-CM (Fig. 3C, column a). As shown in Fig. 3D, the calculated velocity of mitochondrial transport in 2.0 pM rVpr-treated cells was slower than that in C-CM-treated cells (0.10 ± 0.02 μm/s and 0.31 ± 0.04 μm/s, respectively). These results suggest that Vpr induces abnormality in mitochondria transportation through the suppression of ATP synthesis.

To elucidate the effect of mitochondrial transport inhibition in mitochondrial localization, cells treated with serially increasing concentrations of rVpr were stained with antibody against cytochrome *c*, a mitochondrial inner membrane protein. As shown in Fig. 3E, the localization of mitochondria in primary neurites of cells seemed to be altered and reduced when the progenitor cells were treated with rVpr at concentrations above 0.2 pM. Although rVpr did not affect the total mitochondrial content in each live cell as shown by MitoTracker staining (Fig. 3F), the mitochondrial content in neurites of rVpr-treated cells was significantly reduced (Fig. 3G), indicating that the amount of mitochondrial content decreased predominantly within neurites in the presence of rVpr, and this might be caused by the retardation of mitochondrial transportation.

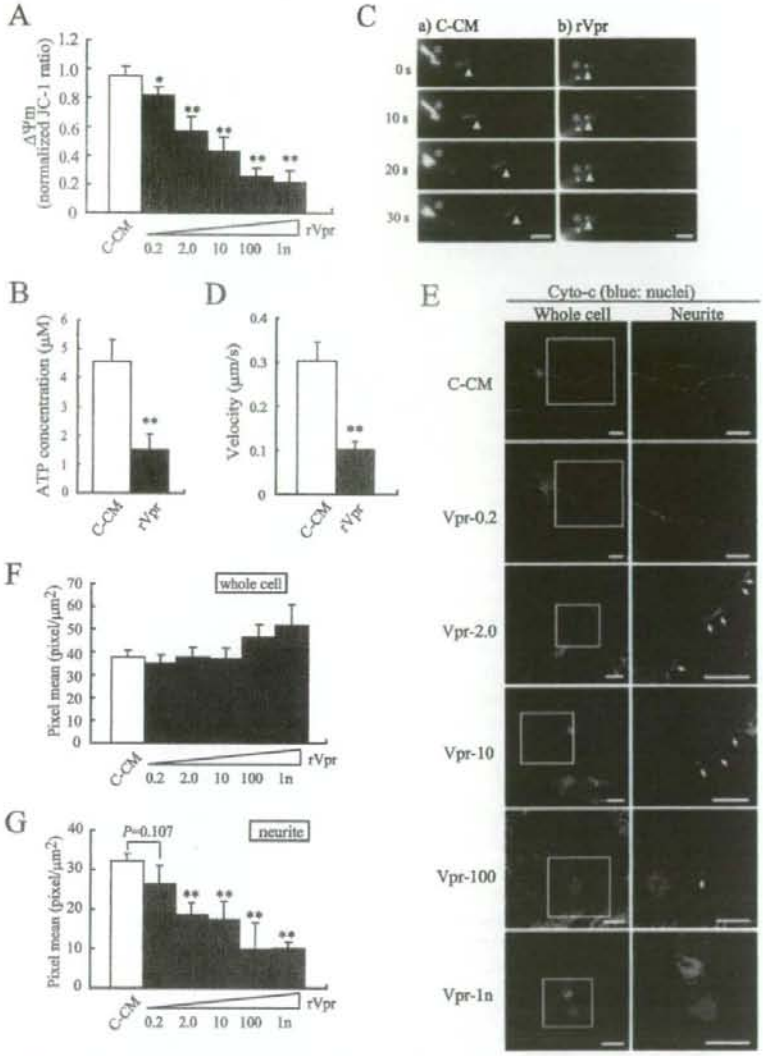

FIG. 3. Mitochondrial dysfunction caused by treatment with Vpr. (A) C-CM, Vpr-0.2, Vpr-2.0, Vpr-10, Vpr-100, and Vpr-1n were added to differentiation cultures of neuronal progenitor cells. Cells cultured in each medium were stained with JC-1, and the $\Delta\Psi m$ was calculated as described in Materials and Methods. *, $P < 0.05$ compared to the results for C-CM culture; **, $P < 0.01$ compared to the results for C-CM culture. (B) The cellular ATP concentration of progenitor cells cultured in C-CM or 2.0 pM rVpr (rVpr) was measured. **, $P < 0.01$ compared to the results of C-CM culture. (C) Neuronal progenitor cells cultured in C-CM (column a) or 2.0 pM rVpr (column b) were stained with MitoTracker. Images were acquired every 10 s using a 63× objective. Asterisks indicate stationary mitochondria, and arrowheads indicate moving mitochondria within neurites. Scale bars, 5 μm. (D) The velocity of mitochondrial transportation within neurites under each condition was calculated as described in Materials and Methods. **, $P < 0.01$ compared to the results for C-CM culture. (E) Mitochondria in progenitor cells cultured in each condition were stained using antibody against cytochrome *c* (Cyto-c; green), and nuclei were stained by Hoechst 33342 (blue), as described in Materials and Methods. Rectangular regions were enlarged and are shown in the right panels. Arrows indicate mitochondrial compartments within neurites. Confocal images were obtained using a 63× objective. Scale bars, 20 μm. (F and G) Progenitor cells treated with or without a serial dilution of rVpr as described above were stained with MitoTracker, and the mean pixels of whole cells (F) or neurites (G) were quantified. **, $P < 0.01$ compared to the results for C-CM culture.

Correlation between rVpr-induced mitochondrial membrane depolarization and developmental retardation of neuronal progenitor cells. We used Vpr recombinant mutants that have a strong, a moderate, or no ability to caused mitochondrial membrane depolarization to study the correlation between Vpr-mediated $\Delta\Psi m$ reduction and developmental arrest. As shown in Fig. 4A, one C-terminal deletion mutant of rVpr protein containing amino acids (aa) 1 to 84 (rVpr-ΔC12),

TABLE 1. Vpr-induced apoptosis in neuronal cells

Condition	Concn of Vpr (pM)	% of neuronal cells expressing activated caspase-3
C-CM	0	5.83 ± 0.97
Vpr-0.2	0.2	6.23 ± 2.04[a]
Vpr-2.0	2	7.12 ± 3.08[a]
Vpr-10	10	8.60 ± 1.80[a]
Vpr-100	100	14.69 ± 2.71[b]
Vpr-1n	1,000	17.33 ± 0.42[b]

[a] There was no significant difference between results for the indicated condition and those for C-CM.
[b] $P < 0.01$ compared to results for C-CM.

which is defective in DNA binding (54), was used, and three point mutants of rVpr were used, including R80A, which moderately induces mitochondrial membrane depolarization (25); I81A, which was used as a negative control; and R73, 77, 80A, which cannot induce mitochondrial membrane depolarization (25). We treated the progenitor cells with each mutant rVpr at 2.0 pM and measured the $\Delta\Psi$m in the treated cells. Although the suppression of $\Delta\Psi$m by rVpr-ΔC12 or rVpr-I81A was similar to that by rVpr-WT, the suppression by rVpr-R80A was clearly less than that by rVpr-WT (Fig. 4B). Furthermore, as shown in Fig. 4B, a triple-amino-acid mutant (rVpr-R73, 77, 80A) did not have any ability to cause mitochondrial membrane depolarization. These results confirmed that R73, R77, and R80 are critical amino acids for the induction of mitochondrial membrane depolarization, as described previously (25).

To determine the correlation between the mitochondrial membrane potential and neuronal development, neuronal progenitor cells treated with those mutants at a constant concentration (2.0 pM) were classified into three developmental stages at 48 h in culture as described in Materials and Methods. As shown in Fig. 4C, the classification profiles of rVpr-ΔC12- and rVpr-I81A-treated cells were almost identical to that of rVpr-WT-treated cells. However, in rVpr-R80A-treated cells, less developmental retardation was found and a significantly higher percentage of cells were in stage 3 compared to that for rVpr-WT-treated cells. Furthermore, in rVpr-R73, 77, 80A-treated cells, no developmental arrest was found, as shown by the very similar classification profile compared to that of the control profile. These results show that there may be a positive correlation between the ability of a Vpr mutant to cause membrane depolarization and its ability to cause developmental arrest.

As shown in Fig. 4D, a small but convincing amount of Vpr was detected in the ANT-containing mitochondrion fraction but not in the cytosolic fraction in neuronal progenitor cells treated with 2.0 pM rVpr-WT. This suggests that Vpr has the tendency to accumulate in mitochondria of neuronal progenitor cells. Similar amounts of rVpr-R73, 77, 80A and rVpr-WT were found to be in the mitochondria of the treated cells. However, no cytoplasmic cytochrome *c* was found in cells treated with a high concentration of rVpr-R73, 77, 80A. In addition, a large amount of cytochrome *c* release was found in cytosolic fractions in cells treated with a high concentration (1.0 nM) of rVpr-WT, but the release of cytochrome *c* was hardly found in cells treated with 2.0 pM of rVpr.

To confirm that the observed effects were indeed caused by rVpr, several Vpr deletion mutant peptides were used at a constant concentration (2.0 pM). The Vpr deletion mutant peptides we used were C45 (aa 53 to 96) (38), C45D18 (aa 53 to 78) (38, 55), LR20 (aa 62 to 81), and LR17 (aa 62 to 78) (Fig. 4A). As shown in Fig. 4B, the $\Delta\Psi$m suppression by C45 and LR20 was similar to that by rVpr-WT, but the suppression by C45D18 and LR17 was clearly weaker. In addition, as shown in Fig. 4C, the developmental classification profiles of C45- and LR20-treated cells were almost identical to that of rVpr-WT-treated cells. However, C45D18- and LR17-treated cells had significantly decreased abilities to induce developmental retardation. These results suggest that Vpr deletion mutant peptides have the same abilities to cause mitochondrial membrane depolarization and developmental retardation that rVpr mutants have. The abilities of the Vpr deletion mutant peptides to cause developmental arrest also were dependent on their ability to cause mitochondrial membrane depolarization.

Protection against rVpr-induced mitochondrial dysfunction by UQ. We found that mitochondrial membrane depolarization might induce the inhibition of neuronal development. To reveal the direct effect of mitochondrial membrane depolarization on neuronal development, neuronal cells were treated with an inhibitor of membrane depolarization along with rVpr-WT. UQ, which is a ubiquinone analogue that protects mitochondrial membranes against depolarization by closing the mitochondrial permeability transition pore (mPTP), was used. First, to confirm the specificity of UQ for the inhibition of membrane depolarization, neuronal cells were treated with FCCP, which induces mitochondrial membrane depolarization and inhibits mitochondrial movement within axons (46), in the presence or absence of UQ. At 48 h of culture, the morphology of cells treated with FCCP was very similar to that of cells treated with 2.0 pM rVpr (data not shown). As shown in Fig. 5A, mitochondrial membrane depolarization was induced in neuronal progenitor cells treated with FCCP (100 μM). In progenitor cells simultaneously treated with FCCP and UQ (100 μM), the mitochondrial membrane potential was clearly sustained. Next, we added UQ to cultures of neuronal progenitor cells treated with rVpr (2.0 pM). UQ protected the progenitor cells against depolarization and significantly restored the membrane potential (Fig. 5A). Although membrane depolarization was suppressed with treatment using UQ, no significant recovery was found in cells treated with the caspase-3 inhibitor z-DEVD-fmk (100 μM) or with ATP (10 μM). Similarly, ATP production was not rescued by treatment using z-DEVD-fmk (2.53 ± 0.43 μM) (Fig. 5B). In contrast, when UQ was used, the ATP concentration (3.06 ± 0.36 μM) was restored to the proximity of the control value (3.64 ± 0.30 μM) (Fig. 5B). Treatment with both UQ and z-DEVD-fmk seemed to increase ATP synthesis, although this increase was not found to be statistically significant compared to ATP synthesis with UQ treatment alone.

We next measured the velocity of the transportation of mitochondria in neurites or axons using MitoTracker. We showed severely suppressed mitochondrial transport within the neurites in rVpr-treated cells (Fig. 3C and D). As shown in Fig. 5C, although the addition of z-DEVD-fmk to rVpr-treated cells could not restore the velocity of mitochondrial transport (0.12 ± 0.02 μm/s), the addition of UQ or both UQ and z-DEVD-fmk to rVpr-treated cells restored the velocity of mitochondrial transport (0.17 ± 0.01 and 0.19 ± 0.02 μm/s, respectively), indicating that the transportation of mitochon-

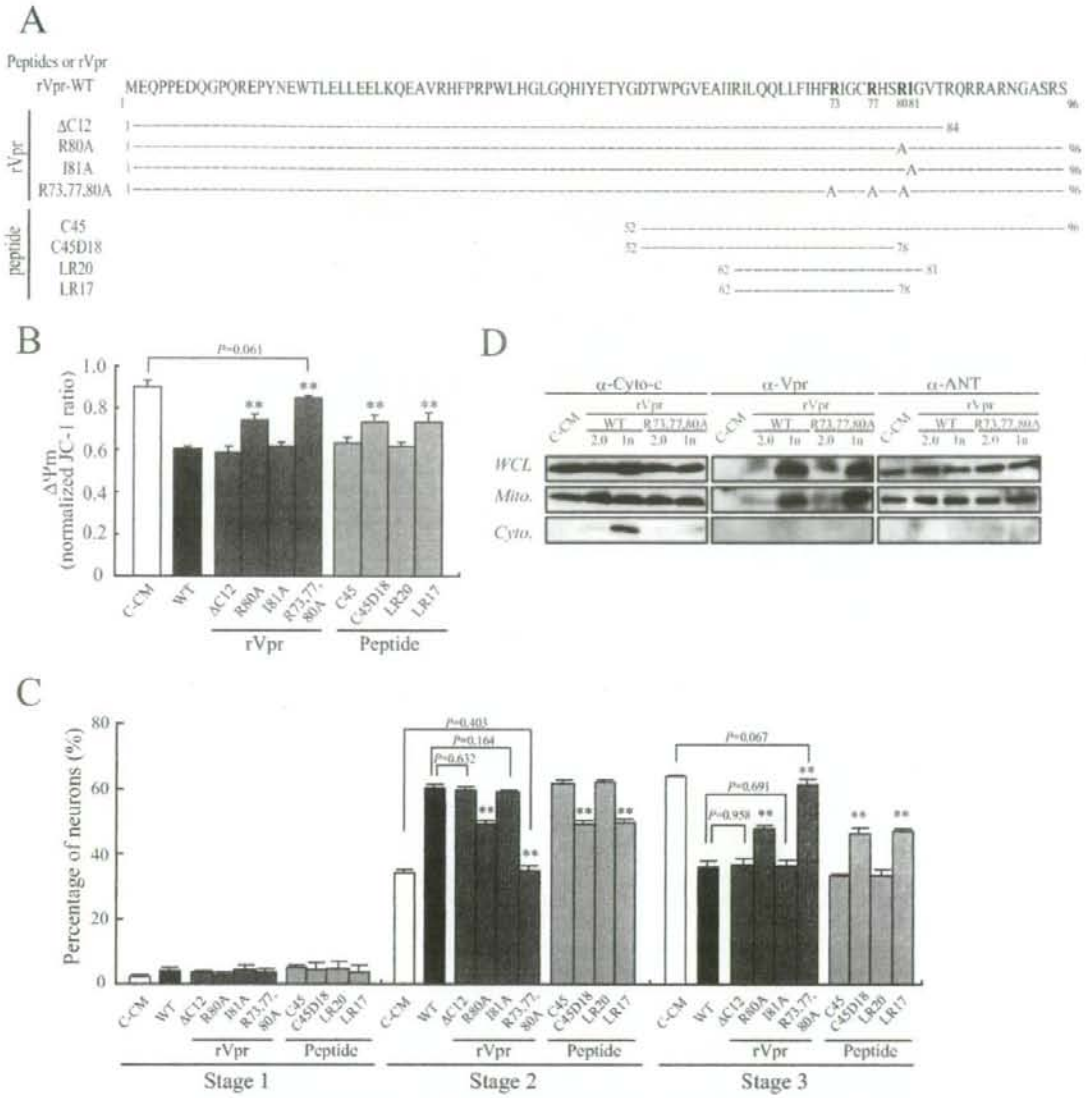

FIG. 4. Inhibition of neuronal development caused by rVpr-induced mitochondrial membrane depolarization. (A) The amino acid sequences of Vpr mutants are displayed. The amino acid sequence of rVpr-WT is depicted at the top. The Vpr deletion mutant peptides and recombinant mutant proteins are listed below, with horizontal lines depicting unaltered sequences and numbers delineating the first or last amino acid of each mutant. The alanines that replace each residue are indicated. (B) Progenitor cells treated with C-CM or with 2.0 pM rVpr-WT (WT), four rVpr mutants (ΔC12; R80A; I81A; and R73, 77, 80A) or four Vpr mutant peptides (C45, C45D18, LR20 and LR17) were stained with JC-1, and the $\Delta\Psi m$ values were calculated as described in the text. **, $P < 0.01$ compared to results for rVpr-WT. (C) Cells cultured in each condition (2.0 pM) were classified into three developmental stages as described above. **, $P < 0.01$ compared to results for rVpr-WT. (D) Cells were cultured in C-CM or rVpr-WT (2.0 pM and 1.0 nM; rVpr-WT-2.0 and rVpr-WT-1n, respectively) or rVpr-R73, 77, 80A (2.0 pM and 1.0 nM; rVpr-R73, 77, 80A-2.0 and rVpr-R73, 77, 80A-1n, respectively). The mitochondrial fraction (*Mito.*) and cytosolic fraction (*Cyto.*) were separated, and anti-cytochrome *c* (α-Cyto-c), anti-Vpr (α-Vpr), or anti-ANT (α-ANT) antibody in individual fractions or whole-cell lysates (*WCL*) was detected by Western blotting using each antibody.

dria within neurites was restored by the treatment of UQ through the restoration of ATP production, followed by the inhibition of mitochondrial membrane depolarization.

To examine the protective capability of UQ against Vpr-induced developmental retardation, neuronal progenitor cells were classified into three developmental stages. When only caspase-3 inhibitor (z-DEVD-fmk) was added to CM of 2.0 pM Vpr-treated cells, the majority of neuronal cells were retained

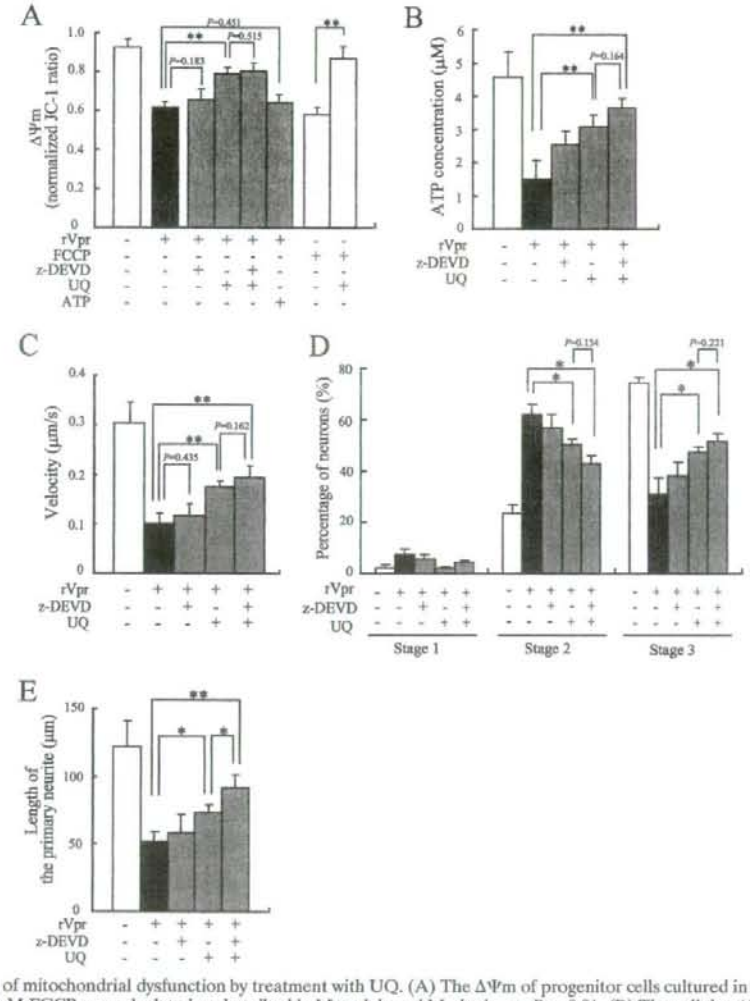

FIG. 5. Restoration of mitochondrial dysfunction by treatment with UQ. (A) The $\Delta\Psi$m of progenitor cells cultured in C-CM or in the presence of 2.0 pM rVpr or 100 μM FCCP was calculated as described in Materials and Methods. **, $P < 0.01$. (B) The cellular ATP concentration of cells cultured in C-CM or in the presence of 2.0 pM rVpr (rVpr) was measured. **, $P < 0.01$. (C) The velocity of mitochondrial transportation within neurites or axons under each condition was calculated. **, $P < 0.01$. (D) Cells cultured under each condition were classified into three developmental stages as described in the text. *, $P < 0.05$. (E) The lengths of the primary neurites of cells cultured under each condition were measured. *, $P < 0.05$; **, $P < 0.01$. In all experiments, 100 μM z-DEVD-fmk (z-DEVD), 100 μM UQ, and 10 μM ATP were used.

at stage 2, as was the case for cells treated with Vpr alone. However, after treatment with UQ or both UQ and z-DEVD-fmk, a significant fraction of Vpr-treated cells proceeded to stage 3 (Fig. 5D), suggesting that the recovery of mitochondrial transportation induced by UQ treatment allowed for the development of neurons. Furthermore, to determine the ability of UQ to restore neurite outgrowth, the length of the primary neurite of neuronal cells was measured at 48 h after the initiation of differentiation. When UQ was added to 2.0 pM Vpr-treated cells, the mean length of primary neurites was significantly longer than that of cells treated with Vpr alone or also with z-DEVD-fmk (Fig. 5E). Interestingly, the rescue of axonal growth was more efficient when UQ and z-DEVD-fmk were added together than when only UQ was added ($P < 0.05$).

Protective effect of UQ on neuronal development in organotypic hippocampal slice cultures. To better simulate the effect of soluble Vpr on neuronal precursor cells in vivo and to characterize the ability of the caspase-3 inhibitor and UQ to rescue neuronal development from Vpr-induced abnormalities, we employed rat organotypic hippocampal slice cultures. In organotypic hippocampal slice cultures, neurons are maintained in microenvironments that are very similar to those found in vivo (17). Not only the extracellular architect but also the synaptodendritic interactions are reconstituted in slice cul-

tures (18). In addition, the presence of neurogenesis has been reported to happen in hippocampal slice cultures (28, 45). For these reasons, slice cultures have been used widely to study the morphology and plasticity of the hippocampus. The typical cellular arrangement of granule cells was reconstituted in slices on porous membranes 14 days after the initiation of culture. Slices then were cocultured with HIV-1_{JRFL}-infected MDM or uninfected MDM across the porous membrane or were exposed to rVpr (2.0 pM). From the examination of B3T, a neuronal cell marker, and NFP expression using immunofluorescence, we found that the number of axons severely decreased in the slices exposed to HIV-1-infected MDM or rVpr (Fig. 6A and B). In addition, in the slices exposed to HIV-1-infected MDM or rVpr, the expression of MAP2, a marker for the neuronal dendritic network, was severely disturbed (Fig. 6A and B). We also found atrophy and the beading of dendrites (Fig. 6A), indicating that postsynaptic structures also were severely disrupted. These results suggest that HIV-1-infected MDM or Vpr induce axonal and dendritic malformation in organotypic hippocampal slice cultures.

Intrinsic and spontaneous neurogenesis are reported to take place at the DG in organotypic hippocampal slice cultures (28, 45). To investigate the dysfunction of neuronal cell development in hippocampal slice cultures exposed to HIV-MDM or rVpr, we labeled endogenous precursor cells in the slices using an EGFP-expressing MLV vector (SRα-EGFP). The virus vector was microinjected into the suprapyramidal region of the GCL as described before (28). Since MLV only infects dividing cells and its DNA is incorporated into the host DNA, only newly divided cells express EGFP. After inoculation with SRα-EGFP, slices were exposed to HIV-1-infected MDM, uninfected MDM, or rVpr in the presence or absence of caspase-3 inhibitor (z-DEVD-fmk), UQ, or both. During daily observations of the inoculated areas under a fluorescent microscope, we found many EGFP-expressing cells (data not shown). The numbers of the EGFP-expressing cells increased for 2 weeks postinoculation in all slices (data not shown). To observe the morphology, the slices were fixed and examined by confocal microscopy. EGFP-expressing cells typically were detected in and around the GCL area. Most cells possessed one elongated axon and several dendrite-like processes in slices cultured with or without uninfected MDM (Fig. 7A, rows a and b). In contrast, in slices exposed to HIV-1-infected MDM or rVpr alone, most $EGFP^+$ cells possessed minor neurites with similar lengths but no prominent axons (Fig. 7A, rows c and d), suggesting that both Vpr released from HIV-1-infected MDM and soluble rVpr induced abnormalities in neuronal development. As shown in Fig. 7A, row e, in slices cultured with rVpr plus z-DEVD-fmk, many EGFP-expressing cells had morphologies similar to those of cells in slices exposed to HIV-1-infected MDM or rVpr alone, suggesting that the effect of Vpr was not due to caspase-3-dependent apoptosis. In rVpr-treated slices cultured in the presence of both z-DEVD-fmk and UQ, more than one-third of the EGFP-expressing cells had a single elongated axon and were $NeuN^{high+}$, which is expressed specifically in the nuclei of mature neurons (Fig. 7B, row c), although most $EGFP^+$ cells had several minor neurites and were $NeuN^{dim+}$ in rVpr-treated slices cultured in the absence (Fig. 7B, row a) or the presence of z-DEVD-fmk (Fig. 7B, row b). Next, $EGFP^+$ cells were categorized into immature neurons or mature neurons by their morphologies and the expression of NeuN. $EGFP^+/NeuN^{dim+}$ cells, which have minor neurites but not extended axons, are classified as immature neurons, and $EGFP^+/NeuN^{high+}$ cells that have one elongated axon and several dendrites are classified as mature neurons. As shown in Fig. 7C, for EGFP-expressing mature neurons in rVpr-treated slices cultured in the presence of UQ or both z-DEVD-fmk and UQ, the percentages of EGFP-expressing mature neurons (33.80% ± 3.02% and 34.64% ± 1.83%, respectively) increased compared to those in rVpr-treated slices cultured with or without z-DEVD-fmk (18.48% ± 3.26% and 18.23% ± 1.78%, respectively). In addition, in HIV-CM-cocultured slices, the percentage of EGFP-expressing mature neurons increased in the presence of both z-DEVD-fmk and UQ (23.35% ± 3.42%) compared to that in slices cocultured with HIV-CM (8.65% ± 2.15%) (Fig. 7C). These results suggest that UQ has a protective effect on neuronal development in organotypic hippocampal slice cultures.

DISCUSSION

Neuronal damage can be caused by various viral or host factors, including viral products, excitotoxins, cytokines, and chemokines released from HIV-1-infected macrophages or microglial cells in HIV-1 encephalopathy (14, 29). Viral products such as HIV-1 gp120, Tat, and Vpr have been shown to be deleterious to neurons and to induce neuronal apoptosis (6, 9, 27, 30, 42). Recently, HIV-1-infected macrophages have been shown to affect neuronal development in a murine model (43), although the factors that affect neuronal development have not been identified and the mechanisms have not been clarified.

We found that HIV-1-infected macrophages produced an inhibitory factor(s) that induced the developmental arrest of neuronal progenitor cells, and we identified Vpr as one of the relevant viral factors (Fig. 1 and 2). Although several lines of evidence suggest that HIV-1 Vpr is a potentially toxic molecule that mediates cell death in mature neurons during HIV-1 infection (27, 42, 49), the influence of HIV-1 Vpr on neuronal development or neuronal plasticity has not been examined. Neuronal development can be divided into five morphological stages. First, cells form lamellipodia (stage 1). After several hours, the neurons form a number of immature neurites (stage 2). One of these minor neurites then begins to extend rapidly, becoming much longer than the other neurites (stage 3). This extended neurite becomes an axon. The other neurites then become mature dendrites (stage 4) and begin to establish dendritic components and to construct premature dendritic spines (stage 5) (4). It has been reported that it takes several days for plated neuronal progenitor cells to enter stage 4 (4). As we observed the cultured progenitors for 72 h, they were not investigated for progression beyond stage 3. We revealed that the majority of progenitor cells could extend primary neurites and proceed from stage 2 to stage 3 after 48 h in culture, although the majority of cells treated with both HIV-CM and recombinant Vpr protein could not extend primary neurites and proceed from stage 2 to stage 3 (Fig. 1 and 2), suggesting that Vpr is the key protein that had affected neuronal developmental arrest and caused the inhibition of axon formation in HIV-1-infected MDM. Although the neuronal developmental arrest was suppressed by treatment with anti-Vpr antibody, the

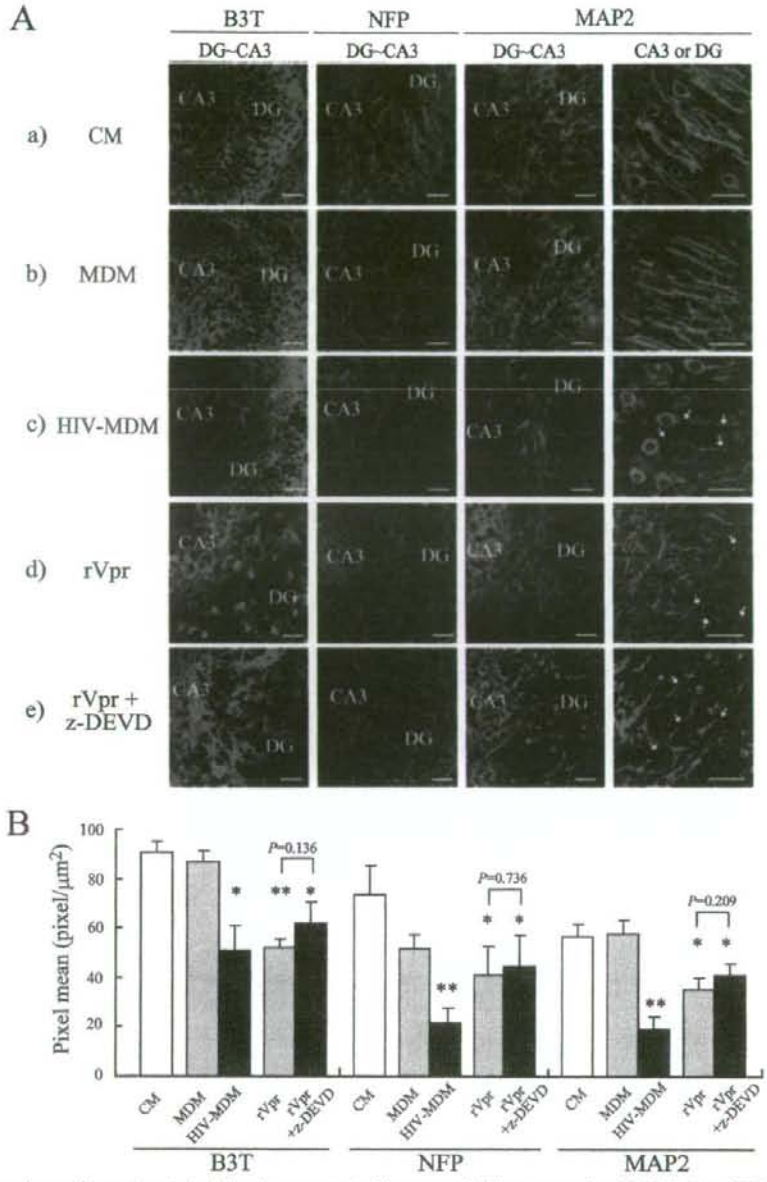

FIG. 6. Axonal disruption and atrophy of dendrites in organotypic hippocampal slices exposed to HIV-1-infected MDM or rVpr. (A) Organotypic hippocampal slices were cocultured alone (a) (CM), uninfected (b) (MDM) or HIV-1-infected MDM (c) (HIV-MDM), or rVpr alone (d) (rVpr) or in the presence of the caspase-3 inhibitor z-DEVD-fmk (e) (rVpr+z-DEVD). Slices were stained with antibodies against B3T, NFP, and MAP2 as described in Materials and Methods. Images were obtained using a 20× objective. Arrows indicate atrophy and the beading of dendrites. CA3, CA3 region of the hippocampus. Scale bars, 50 μm. (B) The mean pixels of the signal in representative areas of the B3T-, NFP-, and MAP2-stained samples shown in panel A were quantified. *, $P < 0.05$ compared to results from culture with CM or MDM (HIV-MDM) or CM (rVpr and rVpr + DEVD-fmk); **, $P < 0.01$ compared to results from culture with CM or MDM (HIV-MDM) or CM (rVpr and rVpr+z-DEVD).

recovery of neuronal development was not complete (Fig. 1E and F). In addition, soluble Vpr protein induced the inhibition of neuronal development in a manner similar to that of HIV-CM, although the effect on developmental retardation apparently was weaker than that of HIV-CM (Fig. 1 and 2). These results suggest that HIV-1-infected macrophages produce other viral proteins or cell-derived humoral factors that also affect neuronal development.

Vpr was found to induce an abnormality in mitochondrial transport at low concentrations through the suppression of

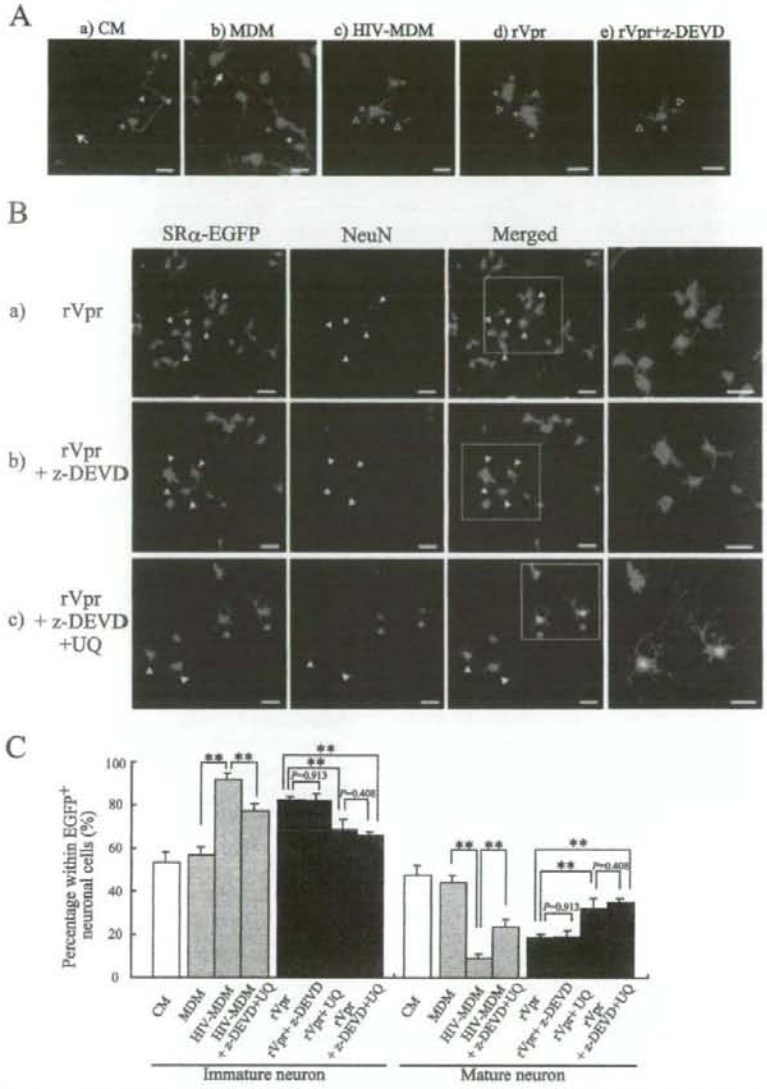

FIG. 7. Protective effect of UQ against Vpr-induced abnormality in neuronal development. (A) Endogenous precursor cells in the slices were labeled by an EGFP-expressing MLV vector, and slices were cocultured in C-CM (a), M-CM (b), HIV-CM (c), or rVpr in the absence (d) (rVpr) or in the presence of the caspase-3 inhibitor z-DEVD-fmk (e) (rVpr+z-DEVD). Arrows indicate axon-like processes. Filled arrowheads indicate dendrite-like processes, and opened arrowheads indicate neurite-like processes. Asterisks indicate neuronal cell bodies. Images were obtained using a 40× objective. Scale bars, 20 μm. (B) EGFP-expressing MLV vector-transduced slices were cultured in the presence of rVpr alone (a) (rVpr), rVpr and z-DEVD-fmk (b) (rVpr+z-DEVD), or rVpr, z-DEVD, and UQ (c) (rVpr+z-DEVD+UQ). Slices were stained with antibody against NeuN (red). Arrowheads indicate immature neurons, and asterisks indicate mature neurons. Rectangular regions were merged and enlarged. Images were obtained using a 40× objective. Scale bars, 20 μm. (C) MLV vector-transduced slices were cultured in CM, MDM, HIV-MDM, and HIV-MDM in the absence or presence of both UQ and z-DEVD-fmk (HIV-MDM+z-DEVD+UQ). Slices also were cultured with rVpr alone (rVpr), rVpr and z-DEVD-fmk (rVpr+z-DEVD), rVpr and UQ (rVpr+UQ), or both (rVpr+z-DEVD+UQ). In all experiments, 2.0 pM rVpr, 100 μM z-DEVD-fmk, and 100 μM UQ were used. $EGFP^+$ cells were classified as mature neurons ($EGFP^+$, $NeuN^{high+}$, and having one elongated axon) or immature neurons ($EGFP^+$, $NeuN^{dim+}$, and having a few neurites). **, $P < 0.01$.

ATP synthesis following mitochondrial membrane depolarization in neuronal progenitor cells (Fig. 3A and B). One of the major functions of mitochondria is to generate an intracellular source of ATP. Neuronal homeostasis is a highly dynamic process marked by an intense need for ATP, as ATP production is critical for the full functioning of motor proteins such as kinesin and dynein (10). As shown in Fig. 3C and D, the reduction of the ATP concentration in rVpr-treated neuronal

progenitor cells appeared to have a direct impact on the velocity of mitochondrial transport. Furthermore, we found significantly smaller amounts of mitochondria in the neurites (Fig. 3E and G), while the amount of mitochondria in whole cells seemed to be unaffected (Fig. 3F). Therefore, the developmental arrest and inhibition of neurite extension that we observed earlier in this study (Fig. 1 and 2) likely were caused by the retarded mitochondrial transport, as mitochondrial transport in neurites has been known to be important for neuronal development (10). Within the CNS, mitochondria are enriched in regions of high metabolic demand, especially in synapses (10, 15, 47). The necessity of mitochondrial transport in neuronal development and homeostasis is becoming clear (10). During neuronal cell differentiation from undifferentiated neuroblasts, cells acquire many neuronal processes. From these processes, axonal and dendritic branches form, and then synaptic connections assemble (10). These highly dynamic processes need large amounts of ATP to be produced at locations where it is needed. Therefore, the appropriate trafficking of mitochondria is a necessary task beginning in the earliest steps of neuronal development (10). To examine the physiological function of mitochondria, such as the maintenance of its membrane potential or ATP synthesis, some mitochondrion-targeted drugs (such as FCCP) previously have been used, and those drugs induced mitochondrial membrane depolarization and inhibited mitochondrial transportation within axons (46). The depolarization of the mitochondrial membrane potential and the inhibition of ATP synthesis caused retardation in mitochondrial transportation (10, 46). Therefore, the suppression of ATP synthesis following mitochondrial membrane depolarization by Vpr induced the retardation of mitochondrial transport into and within neurites, which may have arrested development.

Vpr is well known to induce apoptosis when a high concentration of Vpr is supplemented in culture or is exogenously expressed in cells (26, 27, 39, 41). It has been shown recently that Vpr induces cell cycle arrest following its binding to a large complex consisting of DDB1, Cul4A E3 ubiquitin ligase, and DDB1-Cul4A-associated factor 1 (8, 12, 13, 24, 33, 56, 59). Furthermore, synthetic Vpr peptides are found to directly bind to ANT, a component of the mPTP located on the inner mitochondrial membrane. As a result, a decrease of mitochondria membrane potential and the release of cytochrome *c* are thought to induce the intrinsic apoptosis pathway (25, 26, 48). As shown in Fig. 3A, high concentrations of rVpr (100 pM and 1.0 nM) induced the severe depression of $\Delta\Psi$m in progenitor cells, and the percentage of caspase-3-activated cells was significantly increased (Table 1). In contrast, although low concentrations of rVpr (2.0 and 10 pM) induced the moderate depression of $\Delta\Psi$m, no significant percentage of caspase-3-activated cells was detected. Furthermore, in 1.0 nM rVpr-treated cells, a large amount of cytochrome *c* was released into the cytosol, although cytochrome *c* was hardly released in cells treated with 2.0 pM rVpr (Fig. 4D). These results suggest that high concentrations of rVpr induce apoptosis via the release of cytochrome *c* from mitochondria through the severe reduction of $\Delta\Psi$m. In contrast, probably because a low concentration of rVpr induces a moderate reduction of $\Delta\Psi$m, the release of cytochrome *c* and apoptosis did not take place. However, the moderate reduction of $\Delta\Psi$m caused by treatment with a low concentration of rVpr is able to induce neuronal developmental arrest.

It has been reported that a Vpr peptide (aa 71 to 82) directly binds ANT in vitro, and the critical amino acids for the binding were mapped to three residues, R73, R77, and R80. Mitochondrial membrane depolarization was not caused by Vpr mutants that lacked those amino acids or carried their point mutations (25, 26). As shown in Fig. 3A, we showed that soluble Vpr induced mitochondrial membrane depolarization in neuronal progenitor cells in a dose-dependent manner. As suspected, a Vpr mutant that had mutations at the critical amino acids for its binding to ANT and that had been reported to be incapable of causing mitochondrial membrane depolarization was not able to induce any inhibitory effects on neuronal progenitor cells, including mitochondrial membrane depolarization and the inhibition of neuronal development. In addition, not only rVpr-WT but also the mutant incapable of causing depolarization (rVpr-R73, 77, 80A) were localized at the mitochondrial fraction in neuronal progenitor cells (Fig. 4D). These results suggest that Vpr localizes at the mitochondria and induces the inhibition of neuronal development through mitochondrial membrane depolarization because of the interaction with ANT. In contrast, although rVpr-R73, 77, 80A also localizes at the mitochondria, this mutant may not interact with ANT and induce neuronal developmental arrest.

The mPTP is a large conductance channel of solutes up to 1.5 kDa in size that spans the outer and inner mitochondrial membranes, and the mPTP is composed of the inner membrane ANT, the outer membrane voltage-dependent anion channel, and matrix cyclophilin D. The mPTP frequently is open under pathological conditions such as ATP depletion and mitochondrial membrane depolarization (10, 11). It is possible that the mPTP is opened because of an interaction between ANT and Vpr (25). It has been shown that UQ inhibits mitochondrial depolarization by closing the mPTP through direct interaction at the mPTP binding site (40, 58). Furthermore, recently UQ has been reported to have a protective effect on neurotoxicity in in vivo models of CNS diseases, including Parkinson's diseases, Huntington's disease, and amyotrophic lateral sclerosis, which all involve mitochondrial dysfunction (7). As shown in Fig. 5A, UQ was shown to restore the mitochondrial membrane potential and offer significant protection against rVpr, while the protection by a caspase-3 inhibitor, z-DEVD-fmk, was not statistically significant. In addition, ATP production and mitochondrion transportation was recovered by treatment with UQ but not z-DEVD-fmk (Fig. 5B and C). Even with the presence of z-DEVD-fmk, UQ was able to significantly restore $\Delta\Psi$m, ATP synthesis, and the velocity of mitochondrial transportation. This indicates that the inhibition of neuronal development observed in this study was caused independently of caspase-3-mediated apoptosis.

In HIV-1 encephalopathy, neurocognitive impairment is related to the loss of the synaptodendritic connection (1, 14). Our data demonstrated that not only inhibition of neuronal development but also axonal disruption and atrophy and beading of dendrites were induced by soluble Vpr protein and HIV-1-infected macrophages in organotypic hippocampal slice cultures (Fig. 6 and 7). It was reported that a significant amount of Vpr protein, as high as the nanogram-per-milliliter range, was detected in the CSF of AIDS patients (44). With

some circulating soluble Vpr protein in CNS, Vpr probably causes damage to both mature and immature neurons. Mature neurons may be damaged because of axonal disruption or synaptodendritic injury, and immature neurons may lose the ability to mature. In healthy adult brain, progenitor cells derived from DG of the hippocampus differentiate into mature neurons and are incorporated into the hippocampal circuitry. However, in HIV-1 encephalopathy patients, even when mature neurons are damaged, progenitor cells may not be able to properly differentiate because of the mitochondrial dysfunctions induced by Vpr. This might help the progression of hippocampus-dependent memory loss. Furthermore, we observed that low concentrations of soluble Vpr inhibited neuronal development and induced axonal disruption. It is possible that when low concentrations of Vpr infiltrate into the CNS, focal neuronal damage including axonal disruption and the inhibition of neuronal development are induced even if HIV-1-infected macrophages do not infiltrate into CNS tissues, and this may be a cause of mild neurocognitive disorder. In addition, in the pediatric patients who are affected by HIV-1-associated progressive encephalopathy, neurological dysfunction and developmental delays are seen (52). In the pediatric brain, there are large numbers of neuronal progenitor cells compared to the amount in the adult brain, and our data suggest that Vpr is one of the factors that induces neuronal developmental delay in pediatric patients. Neurotoxic viral and/or cell-derived factors besides Vpr possibly have the potential to induce neuronal developmental retardation, and the pathological process of HIV-1 encephalopathy may be caused by their added effects. To elucidate the pathology of HIV-1 encephalopathy, it is important to identify those factors and to clarify these complicated processes. Our findings suggest that Vpr is one of the important factors that spurs on the progression of HIV-1 encephalopathy.

ACKNOWLEDGMENTS

We thank Naoko Misawa and Chuanyi Nie for support in our study.

This work was supported by a Grant-in-Aid for Scientific Research on Priority Areas from the Ministry of Education, Culture, Sports, Sciences, and Technology of Japan and by grants for research on HIV-AIDS and health science from the Ministry of Health, Labor, and Welfare of Japan.

REFERENCES

1. **Adle-Biassette, H., F. Chretien, L. Wingertsmann, C. Hery, T. Ereau, F. Scaravilli, M. Tardieu, and F. Gray.** 1999. Neuronal apoptosis does not correlate with dementia in HIV infection but is related to microglial activation and axonal damage. Neuropathol. Appl. Neurobiol. **25:**123–133.
2. **Adle-Biassette, H., Y. Levy, M. Colombel, F. Poron, S. Natchev, C. Keohane, and F. Gray.** 1995. Neuronal apoptosis in HIV infection in adults. Neuropathol. Appl. Neurobiol. **21:**218–227.
3. **An, D. S., K. Morizono, Q. X. Li, S. H. Mao, S. Lu, and I. S. Chen.** 1999. An inducible human immunodeficiency virus type 1 (HIV-1) vector which effectively suppresses HIV-1 replication. J. Virol. **73:**7671–7677.
4. **Arimura, N., and K. Kaibuchi.** 2007. Neuronal polarity: from extracellular signals to intracellular mechanisms. Nat. Rev. Neurosci. **8:**194–205.
5. **Azuma, A., A. Matsuo, T. Suzuki, T. Kurosawa, X. Zhang, and Y. Aida.** 2006. Human immunodeficiency virus type 1 Vpr induces cell cycle arrest at the G_1 phase and apoptosis via disruption of mitochondrial function in rodent cells. Microbes Infect. **8:**670–679.
6. **Bachis, A., S. A. Aden, R. L. Nosheny, P. M. Andrews, and I. Mocchetti.** 2006. Axonal transport of human immunodeficiency virus type 1 envelope protein glycoprotein 120 is found in association with neuronal apoptosis. J. Neurosci. **26:**6771–6780.
7. **Beal, M. F.** 2004. Mitochondrial dysfunction and oxidative damage in Alzheimer's and Parkinson's diseases and coenzyme Q10 as a potential treatment. J. Bioenerg. Biomembr. **36:**381–386.
8. **Belzile, J. P., G. Duisit, N. Rougeau, J. Mercier, A. Finzi, and E. A. Cohen.** 2007. HIV-1 Vpr-mediated G2 arrest involves the DDB1-CUL4A(VPRBP) E3 ubiquitin ligase. PLoS Pathog. **3:**e85.
9. **Bruce-Keller, A. J., A. Chauhan, F. O. Dimayuga, J. Gee, J. N. Keller, and A. Nath.** 2003. Synaptic transport of human immunodeficiency virus-Tat protein causes neurotoxicity and gliosis in rat brain. J. Neurosci. **23:**8417–8422.
10. **Chang, D. T., and I. J. Reynolds.** 2006. Mitochondrial trafficking and morphology in healthy and injured neurons. Prog. Neurobiol. **80:**241–268.
11. **Crompton, M.** 1999. The mitochondrial permeability transition pore and its role in cell death. Biochem. J. **341:**233–249.
12. **Dehart, J. L., and V. Planelles.** 2007. HIV-1 Vpr links proteasomal degradation and checkpoint activation. J. Virol. doi:10.1128/JVI.01628-07.
13. **DeHart, J. L., E. S. Zimmerman, O. Ardon, C. M. Monteiro-Filho, E. R. Arganaraz, and V. Planelles.** 2007. HIV-1 Vpr activates the G2 checkpoint through manipulation of the ubiquitin proteasome system. Virol. J. **4:**57.
14. **Ellis, R., D. Langford, and E. Masliah.** 2007. HIV and antiretroviral therapy in the brain: neuronal injury and repair. Nat. Rev. Neurosci. **8:**33–44.
15. **Erecińska, M., and I. A. Silver.** 1994. Ions and energy in mammalian brain. Prog. Neurobiol. **43:**37–71.
16. **Eriksson, C., A. Bjorklund, and K. Wictorin.** 2003. Neuronal differentiation following transplantation of expanded mouse neurosphere cultures derived from different embryonic forebrain regions. Exp. Neurol. **184:**615–635.
17. **Gähwiler, B. H.** 1984. Development of the hippocampus in vitro: cell types, synapses and receptors. Neuroscience **11:**751–760.
18. **Gähwiler, B. H., M. Capogna, D. Debanne, R. A. McKinney, and S. M. Thompson.** 1997. Organotypic slice cultures: a technique has come of age. Trends Neurosci. **20:**471–477.
19. **Garden, G. A., S. L. Budd, E. Tsai, L. Hanson, M. Kaul, D. M. D'Emilia, R. M. Friedlander, J. Yuan, E. Masliah, and S. A. Lipton.** 2002. Caspase cascades in human immunodeficiency virus-associated neurodegeneration. J. Neurosci. **22:**4015–4024.
20. **González-Scarano, F., and J. Martin-Garcia.** 2005. The neuropathogenesis of AIDS. Nat. Rev. Immunol. **5:**69–81.
21. **Hollenbeck, P. J., and W. M. Saxton.** 2005. The axonal transport of mitochondria. J. Cell Sci. **118:**5411–5419.
22. **Horton, A. C., and M. D. Ehlers.** 2003. Neuronal polarity and trafficking. Neuron **40:**277–295.
23. **Hoshino, S., B. Sun, M. Konishi, M. Shimura, T. Segawa, Y. Hagiwara, Y. Koyanagi, A. Iwamoto, J. Mimaya, H. Terunuma, S. Kano, and Y. Ishizaka.** 2007. Vpr in plasma of HIV type 1-positive patients is correlated with the HIV type 1 RNA titers. AIDS Res. Hum. Retrovir. **23:**391–397.
24. **Hrecka, K., M. Gierszewska, S. Srivastava, L. Kozaczkiewicz, S. K. Swanson, L. Florens, M. P. Washburn, and J. Skowronski.** 2007. Lentiviral Vpr usurps Cul4-DDB1[VprBP] E3 ubiquitin ligase to modulate cell cycle. Proc. Natl. Acad. Sci. USA **104:**11778–11783.
25. **Jacotot, E., K. F. Ferri, C. El Hamel, C. Brenner, S. Druillennec, J. Hoebeke, P. Rustin, D. Metivier, C. Lenoir, M. Geuskens, H. L. Vieira, M. Loeffler, A. S. Belzacq, J. P. Briand, N. Zamzami, L. Edelman, Z. H. Xie, J. C. Reed, B. P. Roques, and G. Kroemer.** 2001. Control of mitochondrial membrane permeabilization by adenine nucleotide translocator interacting with HIV-1 viral protein R and Bcl-2. J. Exp. Med. **193:**509–519.
26. **Jacotot, E., L. Ravagnan, M. Loeffler, K. F. Ferri, H. L. Vieira, N. Zamzami, P. Costantini, S. Druillennec, J. Hoebeke, J. P. Briand, T. Irinopoulou, E. Daugas, S. A. Susin, D. Cointe, Z. H. Xie, J. C. Reed, B. P. Roques, and G. Kroemer.** 2000. The HIV-1 viral protein R induces apoptosis via a direct effect on the mitochondrial permeability transition pore. J. Exp. Med. **191:**33–46.
27. **Jones, G. J., N. L. Barsby, E. A. Cohen, J. Holden, K. Harris, P. Dickie, J. Jhamandas, and C. Power.** 2007. HIV-1 Vpr causes neuronal apoptosis and in vivo neurodegeneration. J. Neurosci. **27:**3703–3711.
28. **Kamada, M., R. Y. Li, M. Hashimoto, M. Kakuda, H. Okada, Y. Koyanagi, T. Ishizuka, and H. Yawo.** 2004. Intrinsic and spontaneous neurogenesis in the postnatal slice culture of rat hippocampus. Eur. J. Neurosci. **20:**2499–2508.
29. **Kaul, M., G. A. Garden, and S. A. Lipton.** 2001. Pathways to neuronal injury and apoptosis in HIV-associated dementia. Nature **410:**988–994.
30. **Kaul, M., and S. A. Lipton.** 1999. Chemokines and activated macrophages in HIV gp120-induced neuronal apoptosis. Proc. Natl. Acad. Sci. USA **96:**8212–8216.
31. **Koyanagi, Y., S. Miles, R. T. Mitsuyasu, J. E. Merrill, H. V. Vinters, and I. S. Chen.** 1987. Dual infection of the central nervous system by AIDS viruses with distinct cellular tropisms. Science **236:**819–822.
32. **Koyanagi, Y., W. A. O'Brien, J. Q. Zhao, D. W. Golde, J. C. Gasson, and I. S. Chen.** 1988. Cytokines alter production of HIV-1 from primary mononuclear phagocytes. Science **241:**1673–1675.
33. **Le Rouzic, E., N. Belaidouni, E. Estrabaud, M. Morel, J. C. Rain, C. Transy, and F. Margottin-Goguet.** 2007. HIV1 Vpr arrests the cell cycle by recruiting DCAF1/VprBP, a receptor of the Cul4-DDB1 ubiquitin ligase. Cell Cycle **6:**182–188.
34. **Levy, D. N., Y. Refaeli, R. R. MacGregor, and D. B. Weiner.** 1994. Serum Vpr

regulates productive infection and latency of human immunodeficiency virus type 1. Proc. Natl. Acad. Sci. USA **91:**10873–10877.
35. **Lledo, P. M., M. Alonso, and M. S. Grubb.** 2006. Adult neurogenesis and functional plasticity in neuronal circuits. Nat. Rev. Neurosci. **7:**179–193.
36. **Mattson, M. P.** 2007. Mitochondrial regulation of neuronal plasticity. Neurochem. Res. **32:**707–715.
37. **Mattson, M. P., and J. Partin.** 1999. Evidence for mitochondrial control of neuronal polarity. J. Neurosci. Res. **56:**8–20.
38. **Mizoguchi, L, Y. Ooe, S. Hoshino, M. Shimura, T. Kasahara, S. Kano, T. Ohta, F. Takaku, Y. Nakayama, and Y. Ishizaka.** 2005. Improved gene expression in resting macrophages using an oligopeptide derived from Vpr of human immunodeficiency virus type-1. Biochem. Biophys. Res. Commun. **338:**1499–1506.
39. **Muthumani, K., D. S. Hwang, B. M. Desai, D. Zhang, N. Dayes, D. R. Green, and D. B. Weiner.** 2002. HIV-1 Vpr induces apoptosis through caspase 9 in T cells and peripheral blood mononuclear cells. J. Biol. Chem. **277:**37820–37831.
40. **Papucci, L., N. Schiavone, E. Witort, M. Donnini, A. Lapucci, A. Tempestini, L. Formigli, S. Zecchi-Orlandini, G. Orlandini, G. Carella, R. Brancato, and S. Capaccioli.** 2003. Coenzyme Q10 prevents apoptosis by inhibiting mitochondrial depolarization independently of its free radical scavenging property. J. Biol. Chem. **278:**28220–28228.
41. **Patel, C. A., M. Mukhtar, and R. J. Pomerantz.** 2000. Human immunodeficiency virus type 1 Vpr induces apoptosis in human neuronal cells. J. Virol. **74:**9717–9726.
42. **Piller, S. C., P. Jans, P. W. Gage, and D. A. Jans.** 1998. Extracellular HIV-1 virus protein R causes a large inward current and cell death in cultured hippocampal neurons: implications for AIDS pathology. Proc. Natl. Acad. Sci. USA **95:**4595–4600.
43. **Polnektova, L., V. Meyer, L. Walters, X. Paez, and H. E. Gendelman.** 2005. Macrophage-induced inflammation affects hippocampal plasticity and neuronal development in a murine model of HIV-1 encephalitis. Glia **52:**344–353.
44. **Pomerantz, R. J.** 2004. Effects of HIV-1 Vpr on neuroinvasion and neuropathogenesis. DNA Cell Biol. **23:**227–238.
45. **Raineteau, O., L. Rietschin, G. Gradwohl, F. Guillemot, and B. H. Gahwiler.** 2004. Neurogenesis in hippocampal slice cultures. Mol. Cell Neurosci. **26:** 241–250.
46. **Rintoul, G. L., A. J. Filiano, J. B. Brocard, G. J. Kress, and I. J. Reynolds.** 2003. Glutamate decreases mitochondrial size and movement in primary forebrain neurons. J. Neurosci. **23:**7881–7888.
47. **Rowland, K. C., N. K. Irby, and G. A. Spirou.** 2000. Specialized synapse-associated structures within the calyx of Held. J. Neurosci. **20:**9135–9144.
48. **Sabbah, E. N., S. Druillennec, N. Morellet, S. Bouaziz, G. Kroemer, and B. P. Roques.** 2006. Interaction between the HIV-1 protein Vpr and the adenine nucleotide translocator. Chem. Biol. Drug Des. **67:**145–154.
49. **Sabbah, E. N., and B. P. Roques.** 2005. Critical implication of the (70–96) domain of human immunodeficiency virus type 1 Vpr protein in apoptosis of primary rat cortical and striatal neurons. J. Neurovirol. **11:**489–502.
50. **Sacktor, N., M. P. McDermott, K. Marder, G. Schifitto, O. A. Selnes, J. C. McArthur, Y. Stern, S. Albert, D. Palumbo, K. Kieburtz, J. A. De Marcaida, B. Cohen, and L. Epstein.** 2002. HIV-associated cognitive impairment before and after the advent of combination therapy. J. Neurovirol. **8:**136–142.
51. **Schröfelbauer, B., Y. Hakata, and N. R. Landau.** 2007. HIV-1 Vpr function is mediated by interaction with the damage-specific DNA-binding protein DDB1. Proc. Natl. Acad. Sci. USA **104:**4130–4135.
52. **Schwartz, L., and E. O. Major.** 2006. Neural progenitors and HIV-1-associated central nervous system disease in adults and children. Curr. HIV Res. **4:**319–327.
53. **Shors, T. J., G. Miesegaes, A. Beylin, M. Zhao, T. Rydel, and E. Gould.** 2001. Neurogenesis in the adult is involved in the formation of trace memories. Nature **410:**372–376.
54. **Tachiwana, H., M. Shimura, C. Nakai-Murakami, K. Tokunaga, Y. Takizawa, T. Sata, H. Kurumizaka, and Y. Ishizaka.** 2006. HIV-1 Vpr induces DNA double-strand breaks. Cancer Res. **66:**627–631.
55. **Taguchi, T., M. Shimura, Y. Osawa, Y. Suzuki, I. Mizoguchi, K. Niino, F. Takaku, and Y. Ishizaka.** 2004. Nuclear trafficking of macromolecules by an oligopeptide derived from Vpr of human immunodeficiency virus type-1. Biochem. Biophys. Res. Commun. **320:**18–26.
56. **Tan, L., E. Ehrlich, and X. F. Yu.** 2007. DDB1 and Cul4A are required for human immunodeficiency virus type 1 Vpr-induced G_2 arrest. J. Virol. **81:** 10822–10830.
57. **van Praag, H., A. F. Schinder, B. R. Christie, N. Toni, T. D. Palmer, and F. H. Gage.** 2002. Functional neurogenesis in the adult hippocampus. Nature **415:**1030–1034.
58. **Walter, L., V. Nogueira, X. Leverve, M. P. Heitz, P. Bernardi, and E. Fontaine.** 2000. Three classes of ubiquinone analogs regulate the mitochondrial permeability transition pore through a common site. J. Biol. Chem. **275:**29521–29527.
59. **Wen, X., K. M. Duus, T. D. Friedrich, and C. M. de Noronha.** 2007. The HIV1 protein Vpr acts to promote G2 cell cycle arrest by engaging a DDB1 and Cullin4A-containing ubiquitin ligase complex using VprBP/DCAF1 as an adaptor. J. Biol. Chem. **282:**27046–27057.

Significant Virus Replication in Langerhans Cells following Application of HIV to Abraded Skin: Relevance to Occupational Transmission of HIV[1]

Tatsuyoshi Kawamura,* Yoshio Koyanagi,‡ Yuumi Nakamura,* Youichi Ogawa,* Atsuya Yamashita,† Taku Iwamoto,* Masahiko Ito,† Andrew Blauvelt,§¶ and Shinji Shimada[2]*

The cellular events that occur following occupational percutaneous exposure to HIV have not been defined. In this study, we studied relevant host cellular and molecular targets used for acquisition of HIV infection using split-thickness human skin explants. Blockade of CD4 or CCR5 before R5 HIV application to the epithelial surface of skin explants completely blocked subsequent HIV transmission from skin emigrants to allogeneic T cells, whereas preincubation with C-type lectin receptor inhibitors did not. Immunomagnetic bead depletion studies demonstrated that epithelial Langerhans cells (LC) accounted for >95% of HIV dissemination. When skin explants were exposed to HIV variants engineered to express GFP during productive infection, GFP$^+$ T cells were found adjacent to GFP$^+$ LC. In three distinct dendritic cell (DC) subsets identified among skin emigrants (CD1a$^+$langerin$^+$DC-specific intercellular adhesion molecule grabbing non-integrin (SIGN)$^-$ LC, CD1a$^+$langerin$^-$DC-SIGN$^-$ dermal DC, and CD1a$^-$langerin$^-$DC-SIGN$^+$ dermal macrophages), HIV infection was detected only in LC. These results suggest that productive HIV infection of LC plays a critical role in virus dissemination from epithelium to cells located within subepithelial tissue. Thus, initiation of antiretroviral drugs soon after percutaneous HIV exposure may not prevent infection of LC, which is likely to occur rapidly, but may prevent or limit subsequent LC-mediated infection of T cells. *The Journal of Immunology*, **2008, 180: 3297–3304.**

Occupational exposures place health-care personnel (HCP)[3] at risk for infection with blood-borne pathogens via sharps injuries, exposure of mucous membranes, or contact with nonintact skin (e.g., exposed skin that is chapped, abraded, or dermatitic) (1). In prospective studies of HCP, the average risk of HIV transmission after a single percutaneous exposure to HIV-infected blood has been estimated to be 0.3% (2). Although episodes of HIV transmission after exposure to nonintact skin have been documented (3), the average risk for transmission by this route has not been precisely quantified (1). Epidemiologic and laboratory studies suggest that several factors increase the risk of HIV transmission after an occupational exposure, including contact with a device visibly contaminated with the patient's blood, contact with a needle that was in a vein or artery, exposure to hollow-bore needles, a deep injury, and exposure to R5 strains of HIV that use CCR5 for cell entry (1).

Genetic studies have shown that individuals homozygous for a 32-nt deletion in the chemokine receptor CCR5, *CCR5Δ 32*, are protected from primary HIV infection despite numerous exposures (4–7). The importance of CCR5 as a critical coreceptor involved in the sexual transmission of HIV is also supported by the observation that the majority of HIV strains isolated from patients shortly after primary infection are R5 viruses (8–10). In addition, topical application of high doses of the N terminus-modified chemokine Na-nonanoyl[thioproline2, cyclohexylglycine3]RANTES (PSC-RANTES) provided full protection against intravaginal chimeric SIV/HIV challenge in female rhesus macaques, suggesting a critical role for CCR5-mediated infection-dependent pathways in HIV entry (11).

In a primate model of SIV infection, there is controversy regarding which cells in the genital mucosa are initially infected with SIV. Studies have demonstrated that the primary infected cells present in the lamina propria of the cervicovaginal mucosa 48–72 h after intravaginal exposure to SIV are T cells or submucosal dendritic cells (DC), but not epithelial Langerhans cells (LC) (12, 13). When vaginal tissue was examined within 18 h following vaginal inoculation, however, up to 90% of the SIV-infected cells were LC (14). These conflicting observations may be the result of SIV-infected LC emigrating from epithelium relatively soon after viral exposure.

DC-specific intercellular adhesion molecule grabbing non-integrin (DC-SIGN), a C-type lectin receptor (CLR) expressed on dermal macrophages and monocyte-derived DC (MDDC) (15, 16), has been shown to bind HIV gp120 and to facilitate HIV infection of T cells in *trans* (16, 17). Although results from other studies indicate a minor contribution by DC-SIGN in the transmission of HIV from MDDC to T cells (18, 19), DC-SIGN may be involved in viral dissemination. In addition, langerin, an LC-specific CLR, and the mannose receptor, which is expressed on dermal DC, have

*Departments of Dermatology and †Microbiology, Faculty of Medicine, University of Yamanashi, Yamanashi, Japan; ‡Laboratory of Viral Pathogenesis, Research Center for AIDS, Institute for Virus Research, Kyoto University, Kyoto, Japan; §Departments of Dermatology and Molecular Microbiology and Immunology, Oregon Health & Science University, Portland, OR 97239; and ¶Dermatology Service, Veterans Administration Medical Center, Portland, OR 97239

Received for publication November 6, 2006. Accepted for publication December 12, 2007.

The costs of publication of this article were defrayed in part by the payment of page charges. This article must therefore be hereby marked *advertisement* in accordance with 18 U.S.C. Section 1734 solely to indicate this fact.

[1] This work was supported in part by a grant from the Ministry of Education and Science of the Japanese government.

[2] Address correspondence and reprint requests to Dr. Shinji Shimada, 1110 Shimokato, Chuo, Yamanashi 409-3898, Japan. E-mail address: sshimada@yamanashi.ac.jp

[3] Abbreviations used in this paper: HCP, health-care personnel; CLR, C-type lectin receptor; DC, dendritic cell; EGFP, enhanced GFP; IRES, internal ribosome entry site; LC, Langerhans cell; MDDC, monocyte-derived DC; PEP, postexposure prophylaxis; PSC-RANTES, Na-nonanoyl[thioproline2, cyclohexylglycine3]RANTES; DC-SIGN, DC-specific intercellular adhesion molecule grabbing non-integrin; $TCID_{50}$, 50% tissue culture infecting dose.

been shown to bind HIV gp120 (20), suggesting their participation in virus transmission from DC to T cells. In addition, CLR may also enhance de novo CD4/coreceptor-dependent infection of DC (21). The cooperation of CLR and CD4/HIV coreceptors in facilitating de novo infection of DC has been termed *cis* infection (19–21).

To understand how HIV traverses the skin and genital mucosa, we recently developed an ex vivo model in which epithelial tissue explants obtained from suction blister roofs were exposed to HIV (22). By contrast to the studies using MDDC, results from this model indicated that resident LC transmit HIV to T cells via a CD4/CCR5-mediated infection-dependent pathway, and not by CLR-mediated capture pathways (23, 24). LC infection levels in this model correlated with host *CCR5* genotype (e.g., *CCR5Δ 32*), and the genetic susceptibility of LC to HIV infection paralleled genetic susceptibility to HIV in cohorts of HIV-infected individuals (23). These results, along with the finding that immature resident LC express surface CCR5, but not surface CXCR4 (25), suggest that selective R5 HIV transmission observed in epidemiologic studies most likely occurs at the level of the LC. This has been referred to as the primary gatekeeper model.

In our current study, we have modified our previous explant model to focus more on the cellular mechanisms that may be involved following occupational HIV exposure to nonintact skin. HIV was applied to the abraded epithelial surfaces of split-thickness skin explants, and infection of all the possible cell types present in skin was studied in detail.

Materials and Methods

Reagents and Abs

All mAbs were purchased from BD Biosciences, except for anti-p24 mAb and anti-langerin mAb (Beckman Coulter), and anti-DC-SIGN mAb (R&D Systems). Mannan and mannose were purchased from Sigma-Aldrich. R. Offord (University of Geneva, Geneva, Switzerland) provided PSC-RANTES (a newer, more potent analog of RANTES) (26). N. Yamamoto (Tokyo Medical and Dental University, Tokyo, Japan) provided KRH-1636, a small molecule CXCR4 antagonist that blocks X4 HIV-1 entry into target cells (27).

Viruses

Purified, pelleted, and titered $HIV_{Ba\text{-}L}$, an R5 HIV laboratory isolate, stock containing $10^{7.17}$ median tissue culture infectious doses ($TCID_{50}$)/ml was purchased from Advanced Biotechnologies. rHIV-1 expressing GFP (X4 HIV: NL-EGFP; R5 HIV: $NLCSF_{V3}EGFP$ and JRFL-EGFP) were prepared, as previously described (28, 29). Briefly, the X4 HIV-1 expressing GFP (NL-EGFP) was constructed from pNL4-3 by inserting an enhanced GFP (EGFP) gene and an internal ribosome entry site (IRES) sequence between gp41 and the *nef* sequence by PCR-based subcloning. The ATG codon of EGFP was placed 2 bp downstream of gp41 termination codon, and *nef* expression was rescued from insertion of the IRES sequence. The R5 HIV-1 expressing GFP ($NLCSF_{V3}EGFP$) was constructed by replacing the V3 sequence in the NL-EGFP with the V3 sequence from JRCSF. Another R5 HIV-1 expressing GFP (JRFL-EGFP) was generated through insertion of the EGFP/IRES fragment in pJRFL DNA. Virus stock was made via transfection into 293T cells, and its p24Gag levels in the culture supernatant were measured by ELISA (ZeptoMetrix). The p24Gag amounts for NL43-EGFP, $NLCSF_{V3}EGFP$, and JRFL-EGFP were 540, 305, and 113 ng/ml, respectively. The $TCID_{50}$ was determined by a sensitive 14-day endpoint titration assay using PHA-stimulated PBMC from HIV-seronegative healthy donors. The infectious titers of NL43EGFP, $NLCSF_{V3}EGFP$, and JRFLEGFP were 1.8×10^5, 5.3×10^4, and 1.5×10^4 $TCID_{50}$/ml, respectively.

Virus infection of skin explants ex vivo

Split skin was obtained from HIV-negative healthy donors undergoing plastic or corrective surgery (written consent was obtained from all tissue donors, according to the Local Research Ethics Committee). The epidermal surface of skin was abraded with a wire brush to remove the corneal layer. The skin was stored at 4°C and used within 2 h of collection. Skin explants were prepared by cutting abraded skin into 8.0-mm circular pieces. For infection, skin explants were placed in wells of 24-well plastic plates, and, as previously described (30), 3% agarose was added to confine the inoculates to the epidermis by sealing the surrounding area. Virus was added to the epidermal surface, and the plates were incubated at 37°C for 2 h. In other experiments, virus was added directly to culture medium, and entire skin plants were floated on the culture medium. For some experiments, skin explants were preincubated for 20 min at 37°C with various inhibitors, and then $HIV_{Ba\text{-}L}$ at 1/100 final dilution was added before incubation for an additional 2 h at 37°C. After incubation, skin explants were extensively washed to remove unbound virus and inhibitors. After a wash step, three to five infected skin explants were floated on culture medium, RPMI 1640 (Invitrogen Life Technologies) supplemented with heat-inactivated 10% FCS (Sigma-Aldrich), 2 mM L-glutamine, 10 mM nonessential amino acids, 1× penicillin/streptomycin, 10 mM sodium pyruvate, and 25 mM HEPES, in 6-well plates, with each experimental condition performed in duplicate. In some experiments, skin explants were incubated with Dispase II (2.5 mg/ml; Roche Diagnostics) in RPMI 1640 at 4°C. After 4–6 h, the skin was washed to remove dispase, and using fine forceps, the epidermis was separated from the dermis. Epidermal sheets were then exposed to 100-μl droplets containing $NLCSF_{V3}EGFP$ at 10,000 $TCID_{50}$/ml for 2 h at 37°C, washed to remove unbound virus, and then floated on culture medium to allow migration of LC from the explants. The emigrating cells from epidermal sheets were collected 3 days following HIV exposure.

Assessment of HIV transmission to $CD4^+$ T cells

PBMC were isolated by density centrifugation and enriched for $CD4^+$ T cells by negative selection using a commercially prepared mAb mixture/complement reagent (Lympho-Kwik; One Lambda), according to manufacturer's guidelines. The emigrating cells from explants were collected 3–4 days after HIV exposure, and then cocultured with 2.5×10^6 resting allogeneic $CD4^+$ T cells in an approximate skin cell emigrant/T cell ratio of 1:100. In some experiments, HIV-exposed skin explants were incubated with Dispase II (2.5 mg/ml) in RPMI 1640 at 4°C. After 6 h, the epidermis was separated from the dermis, and both layers were washed in PBS. Epidermal and dermal sheets were floated on culture medium for 3–4 days to allow migration of cells from the separated sheets. Cells emigrating from three epidermal or dermal sheets were collected and washed before adding to $CD4^+$ T cells in coculture. In some experiments, the emigrant cells from HIV-exposed skin explants were incubated with control IgG or mAbs against CD3, HLA-DR, or langerin, followed by sheep anti-mouse Ig-coated magnetic beads (Dynal Biotech), according to the manufacturer's protocol. Negative populations were cocultured with $CD4^+$ T cells, respectively. For detection of secreted HIV p24 protein, supernatants were examined for p24 protein content by ELISA (Beckman Coulter).

Assessment of HIV infection

To quantify numbers of infected cells, cells that spontaneously emigrated from skin explants were collected 3–4 days following HIV exposure, as described above, and analyzed by flow cytometry, as previously described (23). Briefly, skin emigrants were preincubated with mouse anti-CD16 mAb and anti-CD32 mAb in staining buffer (2% mouse serum in HBSS) for 10 min at room temperature to block nonspecific staining. After washing twice with staining buffer, cells were incubated with 10 μg/ml mouse anti-human mAbs against surface molecules for 30 min at 4°C, fixed, and permeabilized with Cytofix/Cytoperm reagents (BD Biosciences) for 20 min at 4°C, and incubated with 10 μg/ml FITC-conjugated rat anti-p24 mAb or isotype control Ab diluted in Perm/Wash (BD Biosciences) containing 2% rat serum for 30 min at 4°C. Cells were then examined by flow cytometry using a FACScan (BD Biosciences). HIV-1 p24 mAb staining of the emigrant cells from uninfected skin showed occasional low positive staining (0–0.08%), confirming the specificity of the HIV-1 p24 staining. In some experiments, HIV-1 expressing GFP was added to the epidermal surface of the skin explants or epidermal sheets, and emigrated cells or coculture with $CD4^+$ T cells were examined under fluorescence microscope using IX70 (Olympus) or processed for flow cytometry. Microscopic images were taken using charge-coupled device camera (VB7000; KEYENCE) and VH-Analyzer (H1A5; KEYENCE). In some experiments, the emigrating cells were labeled with PKH67 Red (Sigma-Aldrich), according to manufacturer's instructions, before adding to $CD4^+$ T cells in coculture.

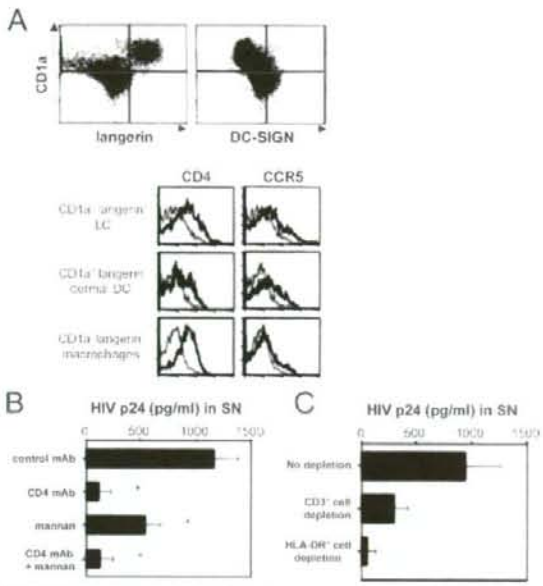

FIGURE 1. After epidermal and dermal exposure to HIV, emigrant cells from HIV-exposed skin transmit infection to T cells. *A*, Emigrating cells from skin explants were stained for the surface Ags shown in combination with HLA-DR staining. Representative data show staining of electronically gated HLA-DR$^+$ cells. An electronic gate was further set on the indicated cell populations in the *upper left panel*, and the expression levels of CD4 and CCR5 in each population are shown (bold line) along with isotype control staining (thin line) (*lower panels*). *B*, Entire skin explants were preincubated with mannan (200 μg/ml) or indicated Abs (40 μg/ml) before exposure to HIV-$1_{Ba\text{-}L}$, and emigrant cells were cocultured with allogeneic CD4$^+$ T cells. *, $p < 0.05$ compared with the control IgG-preincubated explants. *C*, Emigrating cells from HIV-exposed skin explants were collected, and the emigrants were depleted of CD3$^+$ cells or HLA-DR$^+$ cells by immunomagnetic bead separation. Nondepleted or each negative population was cocultured with allogeneic T cells. HIV p24 levels in coculture supernatants (SN) were assessed by ELISA. Data shown represent at least two separate experiments derived from separate donors.

Results

After epidermal and dermal exposure to HIV, DC and T cells that have emigrated from HIV-exposed skin explants transmit virus to CD4$^+$ T cells

During ex vivo culture of skin explants, resident LC, dermal DC, and T cells spontaneously emigrated from explants into surrounding medium in 1–3 days. In experiments in which the numbers of cells emigrating from individual skin explants were determined, the mean cell yield ± SD was 8.4 ± 1.7 × 10^3 (n = 5). The number of cells recovered from the skin explants was similar to that obtained by others (31, 32). We next characterized DC/macrophage subsets migrating from skin explants. HLA-DR$^+$ migratory cells contained three distinct subsets, as follows: CD1a$^+$langerin$^+$DC-SIGN$^-$ LC, CD1a$^+$langerin$^-$DC-SIGN$^-$ dermal DC, and CD1a$^-$ langerin$^-$DC-SIGN$^+$ dermal macrophages, and each subset exhibited comparable surface expression levels of CD4 and CCR5 (Fig. 1*A*).

In initial experiments, $HIV_{Ba\text{-}L}$ (an R5 virus) was added to the entire skin explants, and the emigrating cells from the explants were collected 3–4 days following HIV exposure. As shown in Fig. 1, emigrating cells from HIV-exposed skin explants induced high levels of HIV infection when cocultured with resting allogeneic CD4$^+$ T cells. We could not detect p24 protein in culture supernatants of emigrating cells cultured alone (data not shown), suggesting that the main source of secreted p24 protein in the cocultures was T cells. When anti-CD4 mAb was preincubated with skin explants before HIV exposure, HIV p24 production in the supernatants was substantially inhibited (Fig. 1*B*). By contrast, mannan, a known inhibitor of CLR binding, partially, but significantly inhibited HIV p24 production in the supernatants, and when combined with CD4 mAb did not increase its inhibition provided by CD4 mAb alone (Fig. 1*B*). These data suggest that, after spontaneous epidermal and dermal exposure, transmission of R5 HIV from skin emigrants to T cells is dependent upon a CD4- and CLR-dependent infection process. We then investigated the cell type or types responsible for transmission of virus to T cells. As shown in Fig. 1*C*, HLA-DR$^+$ cells accounted for as much as 95% of HIV-1 dissemination, whereas CD3$^+$ cells contributed partially. These results suggest that HIV-1 dissemination by migratory cells is largely mediated by DC subsets, and DC-T cell conjugates also contribute to the dissemination.

After epidermal exposure to HIV, HIV-infected LC that have emigrated from HIV-exposed skin explants transmit virus to CD4$^+$ T cells

We next tested whether CLR were involved in HIV transmission from skin emigrants to CD4$^+$ T cells after epidermal exposure to HIV. $HIV_{Ba\text{-}L}$ was applied to the surface of abraded skin explants, and the emigrating cells from the explants were collected 3–4 days following HIV exposure. Consistent with previous report (31), abrasion of the epidermal surface had no detectable effect on the phenotype of the emigrant cells (data not shown). As shown in Fig. 2, emigrating cells from HIV-exposed skin explants induced high levels of HIV infection when cocultured with allogeneic CD4$^+$ T cells. We could not detect p24 protein in culture supernatants of emigrating cells cultured alone (data not shown). Interestingly, when PSC-RANTES, a chemically modified RANTES analog and potent CCR5 inhibitor, was preincubated with skin explants before HIV exposure, HIV p24 production in the supernatants was clearly inhibited (Fig. 2, *A* and *B*). By contrast, mannan did not affect HIV p24 production in the supernatants (Fig. 2, *A* and *B*). No cellular toxicity was observed for PSC-RANTES at the doses used in these experiments (24). HIV transmission mediated by skin emigrants was also not affected by preincubation of skin explants with mannose or KRH-1636, a small molecule CXCR4 antagonist (Fig. 2*B* and data not shown). Preincubation of skin explants with CD4 mAb blocked subsequent transmission of $HIV_{Ba\text{-}L}$ to cocultured CD4$^+$ T cells, whereas preincubation with either DC-SIGN mAb or langerin mAb did not affect HIV p24 production in coculture supernatants (Fig. 2*A*). These data suggest that, after epidermal exposure, transmission of R5 HIV from skin emigrants to T cells is totally dependent upon a CD4- and CCR5-dependent and CLR-independent infection process.

We then investigated the cell type or types responsible for transmission of virus to T cells after epidermal exposure to HIV. We first examined the relative contributions of emigrating cells from the epidermis and from the dermis to HIV dissemination. The surface of abraded skin explants was exposed to $HIV_{Ba\text{-}L}$ for 2 h, and the epidermis was then separated from the dermis using dispase. The emigrating cells from the epidermis or dermis were examined for virus carriage to cocultured allogeneic CD4$^+$ T cells. Interestingly, emigrating cells from epidermal, but not dermal, sheets carry HIV (Fig. 2*C*). Consistent with this finding, LC-depleted emigrating cells from HIV-exposed skin explants failed to transmit infection to cocultured T cells (Fig. 2*D*). These results indicate that